

RESEARCH

Open Access



The immunomodulatory effect of oral NaHCO₃ is mediated by the splenic nerve: multivariate impact revealed by artificial neural networks

Milena Rodriguez Alvarez^{1,9*} , Hussam Alkaissi² , Aja M. Rieger³ , Guillem R. Esber⁴ , Manuel E. Acosta⁵, Stacy I. Stephenson⁶ , Allison V. Maurice⁶, Laura Melissa Rodriguez Valencia⁷ , Christopher A. Roman⁸  and Juan Marcos Alarcon⁸ 

Abstract

Stimulation of the inflammatory reflex (IR) is a promising strategy for treating systemic inflammatory disorders. Recent studies suggest oral sodium bicarbonate (NaHCO₃) as a potential activator of the IR, offering a safe and cost-effective treatment approach. However, the mechanisms underlying NaHCO₃-induced anti-inflammatory effects remain unclear. We investigated whether oral NaHCO₃'s immunomodulatory effects are mediated by the splenic nerve. Female rats received NaHCO₃ or water (H₂O) for four days, and splenic immune markers were assessed using flow cytometry. NaHCO₃ led to a significant increase ($p < 0.05$, and/or partial eta squared > 0.06) in anti-inflammatory markers, including CD11bc + CD206 + (M2-like) macrophages, CD3 + CD4 + FoxP3 + cells (Tregs), and Tregs/M1-like ratio. Conversely, proinflammatory markers, such as CD11bc + CD38 + TNFα + (M1-like) macrophages, M1-like/M2-like ratio, and SSC^{high}/SSC^{low} ratio of FSC^{high}CD11bc + cells, decreased in the spleen following NaHCO₃ administration. These effects were abolished in spleen-denervated rats, suggesting the necessity of the splenic nerve in mediating NaHCO₃-induced immunomodulation. Artificial neural networks accurately classified NaHCO₃ and H₂O treatment in sham rats but failed in spleen-denervated rats, highlighting the splenic nerve's critical role. Additionally, spleen denervation independently influenced Tregs, M2-like macrophages, Tregs/M1-like ratio, and CD11bc + CD38 + cells, indicating distinct effects from both surgery and treatment. Principal component analysis (PCA) further supported the separate effects. Our findings suggest that the splenic nerve transmits oral NaHCO₃-induced immunomodulatory changes to the spleen, emphasizing NaHCO₃'s potential as an IR activator with therapeutic implications for a wide spectrum of systemic inflammatory conditions.

Highlights

- Oral sodium bicarbonate (NaHCO₃) intake activates the inflammatory reflex.
- The activating mechanism remains unknown, limiting NaHCO₃'s therapeutic application.
- First-time evidence of NaHCO₃-anti-inflammatory effect is splenic nerve-mediated.
- Decreased granularity of CD11bc + FCS^{high} cells aligns with NaHCO₃'s effect.

*Correspondence:

Milena Rodriguez Alvarez

Milena.rodriguezalvarez@downstate.edu

Full list of author information is available at the end of the article

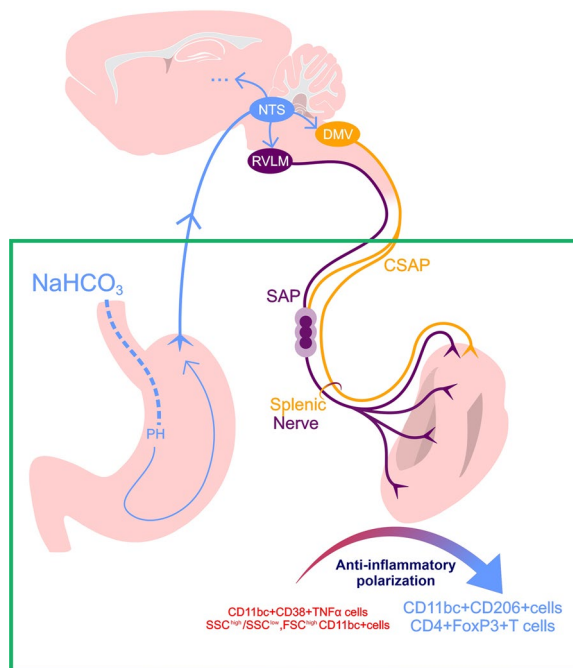


© The Author(s) 2024. **Open Access** This article is licensed under a Creative Commons Attribution 4.0 International License, which permits use, sharing, adaptation, distribution and reproduction in any medium or format, as long as you give appropriate credit to the original author(s) and the source, provide a link to the Creative Commons licence, and indicate if changes were made. The images or other third party material in this article are included in the article's Creative Commons licence, unless indicated otherwise in a credit line to the material. If material is not included in the article's Creative Commons licence and your intended use is not permitted by statutory regulation or exceeds the permitted use, you will need to obtain permission directly from the copyright holder. To view a copy of this licence, visit <http://creativecommons.org/licenses/by/4.0/>. The Creative Commons Public Domain Dedication waiver (<http://creativecommons.org/publicdomain/zero/1.0/>) applies to the data made available in this article, unless otherwise stated in a credit line to the data.

- Selective suppression of CD4+FoxP3+ and CD4-FoxP3+ T cells by spleen denervation

Keywords Inflammatory reflex (IR), Sodium bicarbonate (NaHCO_3), Artificial neural networks, Splenic nerve, Spleen denervation, Cholinergic splenic anti-inflammatory pathway (CSAP), Splanchnic anti-inflammatory pathways (SAP), Vagal nerve stimulation (VNS)

Graphical abstract



Introduction

A common denominator of systemic inflammatory conditions is an excessive systemic inflammatory response (SIR) [68, 78]. A promising new therapeutic field is SIR downregulation by stimulating the inflammatory reflex (IR), the intrinsic physiological neural mechanism that suppresses the production of proinflammatory cytokines [13, 16, 24, 25, 34, 57, 60–62, 70–72, 83, 84, 92]. The most widely explored IR activator is vagal nerve electrostimulation (VNS), which has been successfully used in experimental models of inflammatory disorders in animals and clinical trials in humans [7, 8, 10, 12, 14, 29, 30, 38, 40–42, 46, 56, 81, 87].

Recently, it has been suggested that oral NaHCO_3 intake stimulates IR [65, 66]. This is highly significant because NaHCO_3 is inexpensive, safe, and FDA-approved, ensuring a rapid translation into clinical practice. Oral administration of NaHCO_3 solution in humans and rats induced an anti-inflammatory monocyte polarization relative to controls receiving the

equivalent molar load of NaCl. Flow cytometry analysis in the spleen of NaHCO_3 -treated rats showed an increase in the total number of CD3 + CD4 + FoxP3 + lymphocytes (Tregs) and CD11b + CD206 + IL-10 + macrophages, whereas CD11b + F4/80 + TNF + macrophages decrease [65, 66].

The authors suggested that the immunomodulatory changes induced by oral NaHCO_3 were IR-mediated through cholinergic splenic anti-inflammatory pathways (CSAP) [65, 66]. This was supported by a mitigated NaHCO_3 -mediated anti-inflammatory effect upon spleen displacement in association with the fibrosis of a layer of mesothelial cells attached to the spleen capsule. These cells stain positive for PGP9.5/choline esterase and lay over a dense network of nerves within the spleen capsule, thus, the authors hypothesized that the activation of mesothelial cells, by a yet unknown mechanism, releases acetylcholine near splenic nerve branches triggering CSAP. Nonetheless, spleen displacement may disrupt spleen innervation [23, 26]. Thus, it remains to be determined

whether NaHCO_3 can activate the IR and whether it does so via the activation of cholinergic mesothelial cells, splenic nerve branches, or both.

Here, we generated a sham (SH) and a spleen-denervated (SD) rat model that received four days ad libitum of either NaHCO_3 or water (H_2O). Flow cytometry analysis in the spleen replicated the NaHCO_3 -mediated immunomodulatory effect in SH but not in SD rats. Because both SD and SH models had disrupted connective tissue—hence mesothelial cells' attachment to the spleen capsule—we argue for a necessary role of splenic nerve innervation to bring about NaHCO_3 's effect. Furthermore, SD rats, independently from NaHCO_3 treatment, modulate immunological markers.

Our study sheds light on the gut-brain-spleen communication responsible for NaHCO_3 's effect on immune-cells-driven anti-inflammatory polarization. To the best of our knowledge, this is the first evidence that the immunomodulatory effect induced in the spleen by orally ingested NaHCO_3 is mediated by the splenic nerve.

Methods

Rats

We used 8–12-week-old female (250–325 g, see Additional file 1: Fig. S1a) Sprague Dawley rats from Charles River. They were age-matched for all protocols and housed under standard conditions (12:12-h light–dark cycle and free access to food and water). All studies were conducted in accordance with the National Institutes of Health Guide for the Care and Use of Laboratory. All experiments were conducted under the Institutional Animal Care and Use Committee Animal Use Protocol (IACUC) #20-10574. This protocol was approved by the Office of Animal Welfare, Office of Research Administration from SUNY Downstate Health Sciences University.

Surgeries and spleen collection

Rats underwent spleen denervation [26, 39, 69] confirmed by Western blotting for tyrosine hydroxylase (TH, anti-TH antibody; ab112; Abcam) as previously described [39, 85, 86]. For a description of the spleen denervation, sham surgeries, spleen collection, and immunoblotting see Additional file 1: Fig. S1a.

Rat treatments

After sham ($n=24$) and spleen denervation ($n=16$) surgeries, animals were kept on LS chow with ad libitum water allowing 12–14 days of recovery. On the first day of the experiment, SH and SD rats were randomly assigned to drink a vehicle (H_2O , $n=18$) or 0.1 M NaHCO_3 ($n=22$) freshly made, ad libitum (see Additional file 1: Fig. S1a for daily consumption). This treatment was kept for 4 days, animals were euthanized on day 4 and spleens

were harvested for flow cytometry analysis and western blot.

The concentration for the NaHCO_3 's solution (equivalent to 8.4 mg of NaHCO_3 in 1 L of water) is the highest dose used in rats by Ray et al. [65, 66]. By giving 0.1 M of NaHCO_3 to rats we are below non-toxic levels in humans. A safe dose of NaHCO_3 in chronic kidney disease (CKD) patients is 42 mg/kg/day which is ~ 3000 to 4000 mg of NaHCO_3 daily [22], this amount is equivalent to 12.6 mg in rats. Our animals consumed ~ 0.42 mg of NaHCO_3 per day which is 30 times less than 12.6 mg (non-toxic NaHCO_3 levels in humans). This estimate is based on the amount of water consumed ad libitum by Sprague Dawley rats between 250 and 330 g of weight, which is 50 ml [51]. NaHCO_3 has a molecular mass of 84.004 g/mol, and 50 ml of NaHCO_3 at 0.1 M contains 0.42 mg of NaHCO_3 .

Ray et al. used NaCl at 0.1 M as a vehicle instead of H_2O . We did not use NaCl to avoid the potential proinflammatory confounder effect of hypertonic sodium [33, 91].

Flow cytometry

Tissue processing, antibodies, and technical information

We followed Ray et al. protocol with minor changes [65, 66]. Briefly, harvested spleens were processed and cell suspensions were incubated with antibodies and dead life solution to identify dead cells. For a full description of the flow cytometry protocol see Additional file 1: Fig. S1b, and for reagents and antibodies see Additional file 1: Fig. S2a.

To identify through flow cytometry macrophages residing in the spleen, we used antibodies against CD11bc, CD38, CD206, and $\text{TNF}\alpha$. The CD38 and $\text{TNF}\alpha$ markers have been associated with a proinflammatory phenotype in monocytes and macrophages [31], whereas CD206 is associated with regulatory or anti-inflammatory properties [31]. The denomination of proinflammatory macrophages as M1 or anti-inflammatory as M2 oversimplifies the spectrum of phenotypes observed in these cells and there isn't a nomenclature agreed upon yet [49, 77]. For clarity, in the present work, we describe macrophages as M1-like (CD11bc + CD38 + $\text{TNF}\alpha$ +) and M2-like (CD11bc + CD206 +) as recently suggested [77].

Except for CD38, all the other markers have been used to identify NaHCO_3 -induced changes in rats [65, 66]. Ray et al. used anti-rat F4/80 antibodies for proinflammatory macrophages. At the moment of the current work, Novus had stopped the production of anti-rat F4/80 antibody and there was not a similar product available on the market. CD38 is considered selective for proinflammatory ($\text{LPS}\pm\text{IFN-}\gamma$) but no anti-inflammatory macrophages (IL-4) [5], and transcriptomic analysis identified CD38 as a murine marker able to distinguish proinflammatory

from anti-inflammatory-like macrophages [31]. To identify T cells, we used CD3, for T-helper we added CD4, and for Tregs we used FoxP3. We did not use CD8 but reported that CD4-T cells which include the CD8+ population.

Data acquisition

A Daily QC run was performed using Agilent Flow Cytometer QC particles to ensure the performance parameters meet the requirements. See Additional file 1: Fig. S2b for information about the flow cytometry setup. In flow experiments, the group identifiers were removed, and the analysis was performed by an investigator blind to the source of the samples. In each analysis, 500,000 total events were collected. Compensation beads (Thermo Fisher, Invitrogen™) were used to ensure that median fluorescence intensities of negative and positive were identical. We collected between 30,000 and 40,000 events for compensation. Fluorescence Minus One (FMO) control was used to set the upper boundary for the background signal on the omitted label and to identify and gate the positive population. Samples were analyzed in duplicate measurements. Flow Cytometry was performed at the SUNY Downstate Health Sciences University, Flow Cytometry Facility, which received financial support from the Faculty of Medicine and grants from contributing investigators.

Data analysis

NovoExpress software was used to collect and analyze data. Dead cells and debris were excluded using forward and side scatterplots and dead life staining. Doublets were excluded with forward scatter height (FSC-H) and forward scatter area (FSC-A) plots. Representative gating images for M2-like macrophages and granularity index in SH and SD rats are shown in Fig. 1g while Tregs are shown in Fig. 2e. The granularity index in FSC^{high}/CD11bc cells was determined after identifying two distinct cell populations based on granularity (SSC^{high}/SSC^{low}). After excluding debris and doublets we distinguish the alive populations (Additional file 1: Fig. S3a, gate R3) with lower FSC-A (y-axis) and higher FSC-A values (gate R6). We then assessed the degree of granularity (SSC values, Fig. 1B, y-axis) in both populations. Within R3 we gate agranular (SSC^{low}) cells whereas R6 contained two populations, agranular and granular (SSC^{high}). The cells inside R6 (R8 and R10 gates, Fig. 1g) are CD11bc positive and are the biggest. We identify that R8 contains those more granular cells. A summary of further gating of each cell is in Additional file 1: Fig. S3.

Cells expressing specific markers were reported as the ratio of the percentage of the events from the parent population in a specific quadrant or gate (positive

population), divided by the same number plus the percentage of events from the parent population contained in the quadrant that did not express the marker (negative population). See Additional file 1: Fig. S2c for a detailed description of the proportion rate calculation for each cell type.

Statistical analysis

Data for continuous variables are expressed as means ± standard deviation (SD). We used the Kolmogorov-Smirnov test to assess the normal distribution and we applied log10 transformation to those non-parametric variables (see Table 1). Logarithmic transformation was applied to variables with a non-parametric distribution resulting in a parametric distribution. A two-factor ANOVA was used to compare the four groups (SH surgery drinking H₂O or NaHCO₃, or SD drinking H₂O or NaHCO₃) and assess for interaction between treatment (H₂O or NaHCO₃) and surgery (SH, or SD). The test of single effects was used to discriminate the difference between groups if an interaction was present [32], Support, 2022 #306). One-way ANOVA was used to compare weight at euthanasia and amount of H₂O or NaHCO₃ solution consumption. The Levine test assessed for equal variances (see Table 1). Multivariate analysis was done using Artificial Neural Networks (ANN) and principal component analysis (PCA). We did not assess collinearity in the ANN models because of good predictive capacity in presence of collinearity [88]. We assessed multicollinearity before PCA excluding variables with a variance inflation factor (VIF) above 5 [88].

To assess the magnitude of the difference between variables we used the effect size (ES) and the probability. The ES was measured by the partial eta squared (η^2) and it was labeled “important” when η^2 was above 0.06 (moderate = 0.14 > η^2 > 0.06; high = η^2 > 0.14) [35]. The significance level was defined as $p < 0.05$. We provide both measurements in tables and Figures. All the graphs and data tables were designed using Prism GraphPad, and the statistical analysis was performed with SPSSv28 software.

Results

Effect of oral NaHCO₃ intake in SH and SD animals

SD and SH rats were randomly assigned to drink a vehicle (H₂O), or a solution of NaHCO₃ (0.1 M) ad libitum for 4 continuous days. After spleen processing, immune cell phenotypes were identified by flow cytometry (see Additional file 1: Fig. S3b). Four groups of animals were stratified in 2 factors, surgery (SH or SD) and treatment (H₂O or NaHCO₃). The means and standard deviations for all variables are shown in Table 1. To control

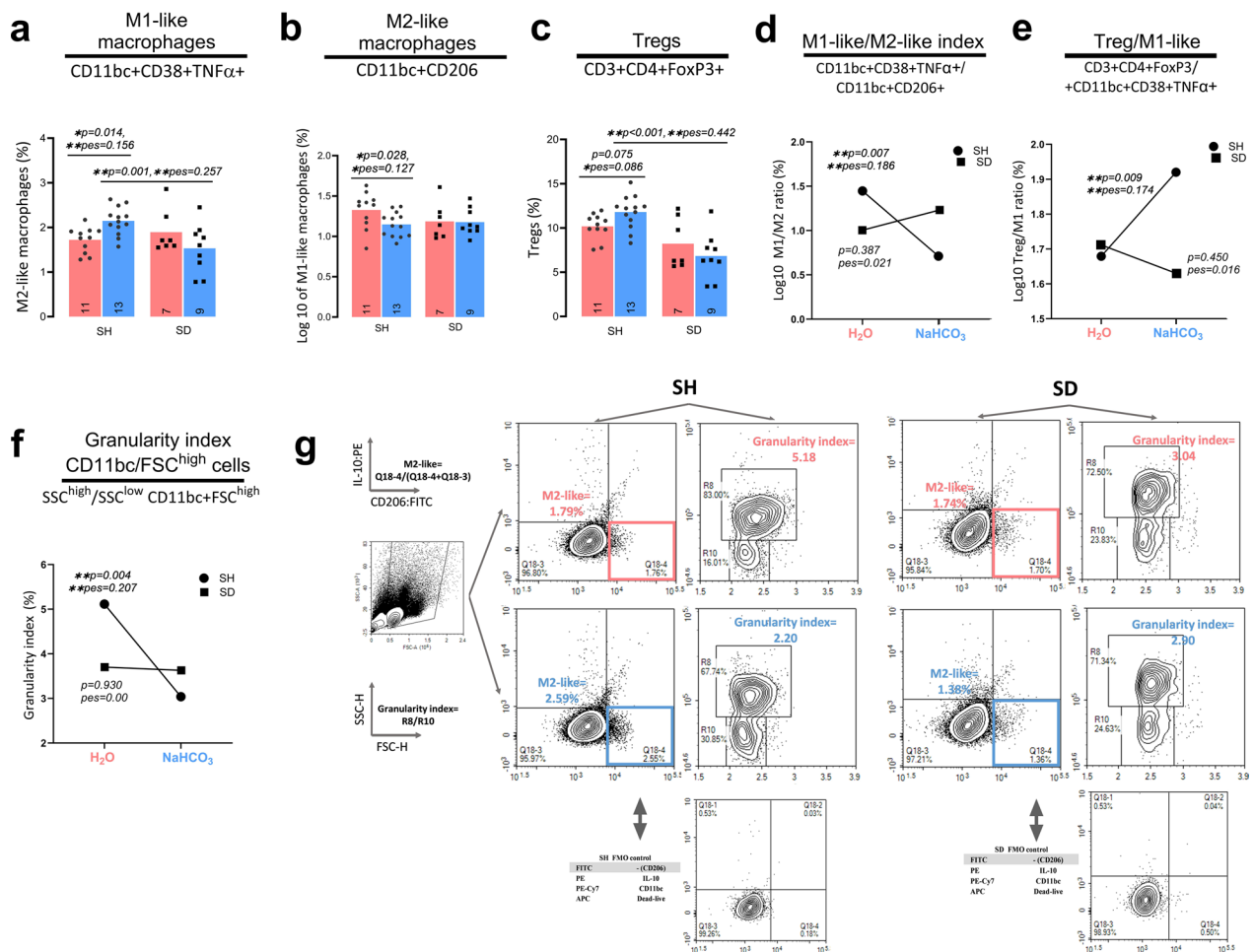


Fig. 1 The immunomodulatory effect induced by oral NaHCO₃ on immune markers is abolished in SD animals. Spleen denervation has an independent immunomodulatory effect. SD and SH rats were randomly assigned to drink H₂O or NaHCO₃, spleen was processed for immunophenotyping by flow cytometry. All values represent the percentage of live cells (an expanded gating for all cells can be seen in Additional file 1: Fig. S2a), with marker positivity listed below cell subtypes. The interaction was evaluated with a two-factor ANOVA (treatment; surgery). The interaction was considered present for *p*<0.15 and *p*se >0.04 and ANOVA was followed by a test of single effects (Table 1). Two-Factor ANOVA results: **a**. CD11bc + CD38 + TNF α + cells, interaction present, *p*=0.137; **b** CD11bc + CD206 + cells, interaction present, *p*=0.006**; **c** CD3 + CD4 + FoxP3 + cells, interaction present, *p*=0.115; **d** M1-like/M2-like index, interaction present, *p*=0.018*; **e** Log10 of the Treg/M1-like index, interaction present, **p*=0.023; **f** SSC^{high}/SSC^{low} of CD11bc + FSC^{high} cells, interaction present, *p*=0.070. The *p* and *p*se values of interest (2-factor ANOVA, and test of simple effects) are listed on each figure if respective group effects were found important (*p*<0.05 and/or *p*se >0.06). Percentages of M1-like and M2-like macrophages and granulinity index are indicated in corresponding quadrants. **g** Representative gating for M2-like macrophages and granulinity index in SH and SD rats, treated with H₂O or NaHCO₃. FMOs control for SH and SD for M2-like macrophages is shown. The colors light red and blue represent H₂O and NaHCO₃, respectively. At the left of the figure is the formula used to calculate macrophages and granulinity index number and the y and x-axis labels. *Significant differences *p*<0.05 or moderate SE (*p*se >0.06); ***p*<0.01 or large SE (*p*se >0.14). Figure created with NovoExpress, and Prism GraphPad

a possible interaction between spleen denervation and treatment response to oral NaHCO₃, we used a two-factor ANOVA.

The variables with interaction (Table 1; *p*<0.15, *p*es >0.04) included CD11bc + CD38 + TNF α + cells (M1-like macrophages), CD11bc + CD206 + cells (M2-like macrophages), log10 of the M1/M2 ratio (M1-like/M2-like ratio), SSC^{high}/SSC^{low} ratio in CD11bc + FSC^{high} cells (granulinity index in CD11bc/

FSC^{high} cells), CD3 + CD4 + FoxP3 + lymphocytes (Tregs), and the ratio of Tregs/M1-like macrophages (Tregs/M1).

Within this group, oral NaHCO₃ decreased the fraction of M1-like macrophages and M1-like/M2-like ratio in SH animals compared to the H₂O-treated group (Fig. 1a, d; stats), crucially, this effect was not observed in NaHCO₃ and H₂O treated-SD animals (Fig. 1e; stats). The granulinity index of CD11bc/FSC^{high} also decreases

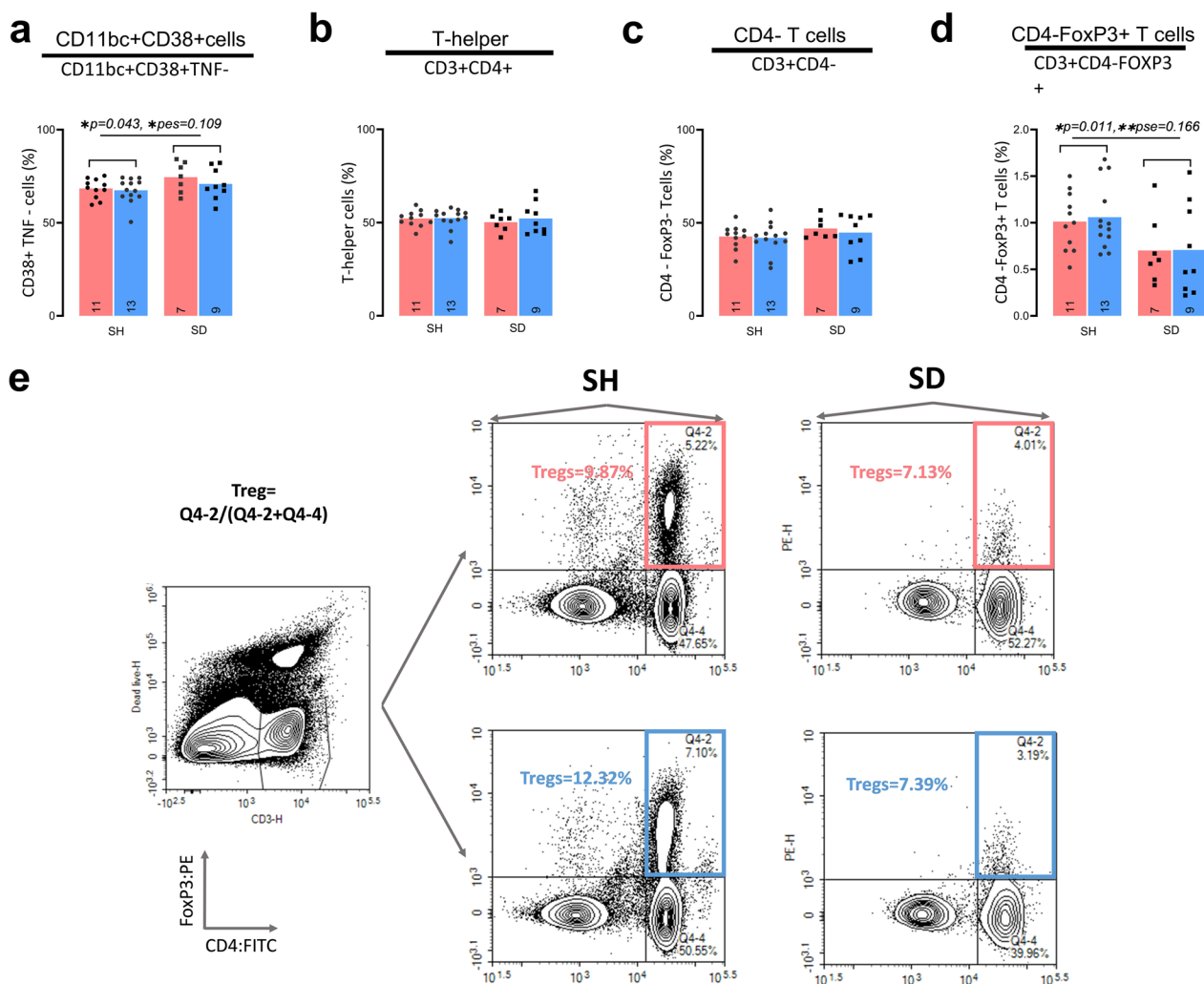


Fig. 2 The $NaHCO_3$ treatment did not impact T-helper, CD11bc + CD38 +, CD4- T cells, and CD4-FoxP3 + T cells. Spleen deveneration increased CD11bc + CD38 + cells and suppressed CD4-FoxP3 + T cells. SD and SH rats were randomly assigned to drink H_2O or $NaHCO_3$, spleen was processed for immunophenotyping by flow cytometry. All values represent the percentage of live cells (an expanded gating for all cells can be seen in Additional file 1: Fig. S2a, b), with marker positivity listed below cell subtypes. The interaction was considered present for $p < 0.15$ and $pse > 0.04$. Two-Factor ANOVA results: **a** CD11bc + CD38 + cells, no interaction $p = 0.559$, treatment $p = 0.317$, surgery $p = 0.043^*$; **b** CD3 + CD4 + cells, no interaction $p = 0.690$, treatment $p = 0.632$, surgery $p = 0.509$; **c** CD3 + CD4 - cells, no interaction $p = 0.777$, treatment $p = 0.564$, surgery $p = 0.168$; **d** CD3 + CD4 - FoxP3 +, no interaction $p = 0.861$, treatment $p = 0.830$, surgery $p = 0.011^*$; The p and pse values of interest (2-factor ANOVA, and test of simple effects) are listed on each figure if respective group effects were important ($p < 0.05$ and/or $pse > 0.06$). **e** Representative gating for Tregs isolated from the spleen of SH and SD rats, treated with H_2O or $NaHCO_3$. The color light red represents H_2O and light blue $NaHCO_3$. To the left is the formula used to calculate Treg's final number and y and x-axis. *Significant differences $p < 0.05$ or moderate ES ($pse > 0.06$); ** $p < 0.01$ or large ES ($pse > 0.14$). Figure created with NovoExpress and Prism GraphPad

in the $NaHCO_3$ -SH group (Fig. 1f; stats), while remaining unchanged in the SD animals (Fig. 1f; stats). This variable decreases in the same direction as proinflammatory monocytes, this is supported by a positive correlation with M1-like and negative with M2-like macrophages (Pearson coefficient 0.723, $p < 0.01$; - 0.522, $p < 0.01$ respectively) without collinearity with either macrophage subtype (Additional file 1: Fig. S5b). In addition, $NaHCO_3$ treatment increased M2-like macrophages, Tregs, and

Tregs/M1-like ratio in SH animals compared to the H_2O group (Fig. 1b, c, e; stats); and like the M1-like findings, the $NaHCO_3$ -induced rise in M2-like, Treg, and Treg/M1-like was not observed in SD animals (Fig. 1b, c, e; stats).

The variables without interaction (Table 1; $p > 0.15$, $pse < 0.04$) between treatment and surgery involve CD11bc + CD38 + cells (CD11bc + CD38 + cells; Fig. 2A), CD3 + CD4 + lymphocytes (T-helper; Fig. 2B), CD3 + but

Table 1 Descriptive statistics, two-factor ANOVA, and test of simple effects analysis for immune markers after immunophenotyping with flow cytometry

Descriptive statistics	CD11bc+CD38+ cells		M1-like macrophage		M2-like macrophage		Granularity index in FSC ^{high} cells		Macrophage polarization ratio		T-helper		Treg		CD4-T cells		CD4-FoxP3+T cells		Treg/M1-like	
	CD11bc+CD38+	Log10 CD11bc+CD38+	CD11bc+CD206+	CD11bc+SSC ^{high} /SSC ^{low}	Log10 M1-like/M2-like	CD11bc+TNFα+	CD11bc+SSC ^{high} /SSC ^{low}	Log10 M1-like/M2-like	Log10 M1-like/M2-like	Log10 CD3+CD4+	CD3+CD4+FoxP3+	CD3+CD4-FoxP3-	Log10 CD3+CD4-FoxP3+	CD3+CD4-FoxP3+	CD3+CD4-FoxP3-	CD3+CD4-FoxP3+	CD3+CD4-FoxP3-	Log10 Treg/M1-like	Log10 Treg/M1-like	
SH H ₂ O (n= 11)	68.44±5.29	1.33±0.23	1.82±0.74	5.22±2.23	1.09±0.27		5.22±2.23	1.09±0.27	2.72±0.36	10.18±1.44	42.61±6.36	1.01±0.31	1.67±0.229							
SH NaHCO ₃ (n= 13)	67.43±6.62	1.15±0.15	2.23±0.43	2.87±0.97	0.82±0.17		2.87±0.97	0.82±0.17	2.72±0.45	11.79±1.86	41.85±8.19	1.06±0.35	1.92±0.15							
SD H ₂ O (n=7)	74.49±8.16	1.18±0.22	1.89±0.49	3.70±2.17	0.92±0.26		3.70±2.17	0.92±0.26	2.68±0.40	8.22±2.84	46.94±5.54	0.70±0.37	1.71±0.28							
SD NaHCO ₃ (n=9)	70.85±8.33	1.18±0.17	1.53±0.55	3.63±1.39	1.02±0.25		3.63±1.39	1.02±0.25	2.71±0.68	6.83±2.61	44.72±10.22	0.71±0.49	1.63±0.21							
Levene's Test, p	0.430	0.607	0.125	0.073	0.443		0.073	0.443	0.083	0.088	0.177	0.350	0.305							
Distribution (KS), p	0.200	0.200	0.200	0.200	0.146		0.200	0.146	0.200	0.132	0.172	0.200	0.200							
Two-factor ANOVA																				
Interaction (T*Sx) p	0.559	0.137	0.005**	0.070	0.018*		0.070	0.018*	0.690	0.038*	0.777	0.861	0.026*							
pes	0.010	0.058	0.202**	0.088*	0.147**		0.088*	0.147**	0.004	0.115*	0.002	0.001	0.131*							
(Tr) F	1.031								0.233		0.339	0.047								
p	0.317								0.632		0.564	0.830								
pes	0.028								0.006		0.009	0.001								
(Sx) F	4.400								0.446		1.980	7.160								
p	0.043*								0.509		0.168	0.011*								
pes	0.109*								0.012		0.052	0.166**								
Test of simple effects																				
(Tr) SH H ₂ OxNaHCO ₃ F		5.245	6.645	9.388	8.238		9.388	8.238		3.366			7.758							
p		0.028*	0.014*	0.004**	0.007**		0.004**	0.007**		0.075			0.009**							
pes		0.127*	0.156**	0.207**	0.186**		0.207**	0.186**		0.086*			0.174**							
(Tr) SD H ₂ OxNaHCO ₃ F		0.006	3.224	0.008	0.765		0.008	0.765		1.669			0.583							
p		0.941	0.081	0.930	0.387		0.930	0.387		0.205			0.450							
pes		0.000	0.082*	0.000	0.021		0.000	0.021		0.044			0.016							

Table 1 (continued)

	CD11bc+CD38+ cells	M1-like macrophage	M2-like macrophage	Granularity index in FSC ^{high} cells	Macrophage polarization ratio	T-helper	Treg	CD4-T cells	CD4-FoxP3+T cells	Treg/M1-like
	CD11bc+CD38+	Log10 CD11bc+CD38+TNFα+	CD11bc+CD206+	CD11bc+SSC ^{high} /SSC ^{low}	Log10 M1-like/M2-like	Log10 CD3+CD4+	CD3+CD4+FoxP3+	CD3+CD4-FoxP3-	CD3+CD4-FoxP3+	Log10 Treg/M1-like
(Sx) H ₂ O SHxSD		2.384	0.798	3.124	2.491		3.565			0.095
p		0.131	0.378	0.086	0.123		0.067			0.760
pes		0.062*	0.022	0.080*	0.065*		0.090*			0.003
(Sx) NaHCO ₃ SHxSD F		0.126	12.431	0.675	3.876		28.519			9.871
p		0.725	0.001**	0.417	0.057		<0.001**			0.003**
pes		0.003	0.257**	0.018	0.097*		0.442**			0.215**

SH, animals with sham surgery; SD, animals with spleen denervation; Tr, treatment either H₂O or NaHCO₃; Sx, surgery either SD or SH; KS, Kolmogorov Smirnov; p, probability (significant for p < 0.05 except for the variables with an interaction between treatment and surgery where p < 0.15); pes, partial eta squared (small = pes < 0.06, medium = 0.06 < pes < 0.14, large = pes > 0.14); Tr, factor treatment which included either H₂O or NaHCO₃; Sx, factor surgery which included; *significant differences p < 0.05 or moderate size effect (pse > 0.06); **p < 0.01 or large SE (pse > 0.14)

CD4 negative lymphocytes (CD4- T cells; Fig. 2c), and lastly CD3+FoxP3+ and CD4 negative lymphocytes (CD4-FoxP3+ T cells, Fig. 2d). None of these variables differed between the groups in response to treatment. Moreover, the T-helper and CD4-T cells were similar across the SH and SD animals for both H₂O and NaHCO₃ groups.

In summary, in the SH animals, treatment with oral NaHCO₃ in comparison with H₂O increased M2-like macrophages, Tregs, and Tregs/M1-like ratio while decreased M1-like macrophages, the granularity index of CD11bc/FSC^{high}, and M1-like/M2-like ratio. Other cells were not affected including T-helper, CD11bc+CD38+ cells, CD4-T cells, and CD4-FoxP3+ T cells. In SD animals, the comparison of these immunological markers between H₂O and NaHCO₃ remained largely unchanged (Table 1, Figs. 2, and 3). Lastly, the interaction between surgery and treatment suggests an independent immunomodulatory effect induced by spleen denervation (Table 1).

Effect of spleen denervation on immune markers.

This immunomodulatory effect of spleen denervation can be better seen by looking at the test of simple effects between SH and SD animals in each treatment group (Table 1). Within the H₂O group, spleen denervation (compared to H₂O/SH) moderately ($0.14 > p > 0.06$) decreases M1-like macrophages, Tregs, and the granularity index of CD11bc/FSC^{high} cells, and did not change M2-like macrophages (Table 1). Within the NaHCO₃ group, there were no changes ($p > 0.05$, and/or $p < 0.06$) between SD and SH animals for M1-like macrophages or the granularity index. Contrary, SD rats have fewer M2-like macrophages and Tregs ($p < 0.05$, $p > 0.14$, Table 1). These findings point to an effect of spleen denervation on immune markers in both H₂O and NaHCO₃-treated animals.

In the absence of an interaction between treatment and surgery (where the simple effect test is unnecessary), spleen denervation globally decreased CD4-FoxP3+ T cells and increased CD11bc+CD38+ cells in comparison to SH animals (Table 1). Other cells were unaffected by the surgery such as T-helper, and CD4-T cells. Overall, these analyses further indicate that spleen denervation, independently of the treatment effect (NaHCO₃ or H₂O), has an immunomodulatory effect.

Identifying the multivariate effect of spleen denervation by artificial neural network (ANN) classification

Our findings are consistent with the immunomodulatory NaHCO₃-mediated effects described by Ray et al. [65]. Crucially, our data shows the abolishment of this effect by spleen denervation. Next, we assess the same

question with a multivariate approach. We assume that if the effect of NaHCO₃ is mediated by the splenic nerve, a classificatory model integrated by multiple immune markers would generate accurate predictions in SH but not in SD animals. To build the model we used ANN [2, 27, 37, 43, 64]. We included those immune markers with an important difference ($p < 0.05$ and/or $p > 0.06$) between NaHCO₃ and H₂O groups in the ANOVA results (Table 1).

The SH group has 11 and 13 animals subjected to H₂O and NaHCO₃ respectively, whereas the SD group has 7 and 9. The models were generated with SPSS running a simultaneous and parallel analysis for SH and SD groups. We ran five multilayer perceptron (MLP) ANN models (ANN1–ANN5) per group (Additional file 1: Fig. S4b, c). 70% of the sample was used to train the ANN models and 30% to test them which makes a rate of 2.3 ($70/30 = 2.3$). All models contained 6 independent variables, and the outcome-dependent variable was treatment (H₂O or NaHCO₃). To explore the overall performance of the ANN models (5 per group) we examined precision, recall, accuracy, and F1-score (HN, 2019).

All ANN models generated in SH performed consistently better than the models in SD animals (Fig. 3a, b). We selected ANN5 (ANN5-SH, and ANN5-SD) because it has the most comparable training and testing partition rates between SH and SD groups and is the closest to a 2.3 ratio (Additional file 1: Fig. S4a). Hence, a sample of 16 SH and 10 SD animals (66.7% and 62.5% respectively) randomly assigned by SPSS was used as the training, leaving aside 8 SH (33.3%) and 6 SD (37.5%) rats to validate ANN5-SH and ANN5-SD respectively (see network information in Additional file 1: Fig. S4b).

Figure 4a, b display the predictive pseudo-probability for ANN5-SH and ANN5-SD. Within the H₂O category, from left to right, the ANN5-SH model correctly classified more animals as drinking water (Fig. 4a; red boxplot in H₂O category) than incorrectly classified them as drinking NaHCO₃ (Fig. 4a; blue boxplot in H₂O category). Consistently, within the NaHCO₃ category, the ANN5-SH model correctly classified animals -with a predicted probability close to 1- as drinking NaHCO₃ (Fig. 4a; blue boxplot in NaHCO₃ category), and marginally incorrectly classified them -with a predicted probability close to zero- as drinking water (Fig. 4a; red boxplot in NaHCO₃ category). In contrast, the ANN5-SD model showed a 0.6 probability of being classified as NaHCO₃ and a 0.4 probability of being classified as H₂O for either category, thus failing to correctly classify animals to each category (Fig. 4b).

The classificatory robustness of ANN5-SH and ANN5-SD was further compared by using the confusion matrix of cases classification, precision, recall, accuracy, F1

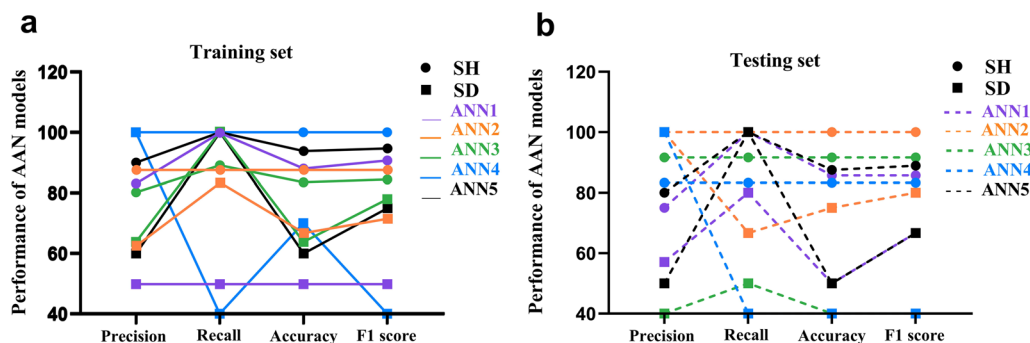


Fig. 3 Measurement tools for all the ANN models. **a** Curves built with precision, recall, accuracy, and F1 score values for the training set are consistently above 80% for SH in comparison with the SD group. **b** Curves built with precision, recall, accuracy, and F1 score values for the testing set are consistently higher for the SH in comparison with the SD group. Figure created with Prism GraphPad

score, and area under the Receiver Operating Characteristics (ROC) curve (AUC), (HN, 2019). A case classification as a confusion matrix for both models is shown in Table 2. The outcome of the ANN models was defined as correct if the predicted probability was above 0.5. ANN5-SH correctly classified 15 out of 16 cases (93.8%) in the training and 7 out of 8 cases (87.5%) in the testing data sample (Table 2). In contrast, ANN5-SD correctly classified 6 out of 10 cases (60%) in the training set and 3 out of 6 cases (50%) in the testing set (Table 2). Thus, the ANN5-SH model performed substantially better than the ANN5-SD to classify treatment exposure, which is consistent with our prediction.

Precision, recall, accuracy, and F1 score for ANN5-SH are above 90% in the training and above 80% in the testing set (Table 3). The F1 score, is above 90% in the training set and 88.9% in the testing set, which is considered very good and good respectively [74]. Contrary, the F1 score for ANN5-SD was lower at 75% and 66.7% (Table 3). Furthermore, ANN5-SH had an accuracy of 93.8% and 87.5% for ANN5-SH, over the 70% considered as good performance in machine learning [93]. In contrast, the accuracy for ANN5-SD was 60% for the training and 50% for the testing set (Table 3). The recall was 100% in the training and testing sets for both groups (Table 3).

The ANN5-SH and ANN5-SD models were further validated by examining the area under the Receiver Operating Characteristics (ROC) curve (AUC), which displays the relationship between true and false positive rates (HN, 2019). The prominent left-shift (from the diagonal representing equal true positive/false positive rate) of the ROC curves in the ANN5-SH model indicates high sensitivity and specificity, and more accurate classification for both the H₂O and NaHCO₃ categories (Fig. 3e). The AUC value, which estimates the quality of the classificatory model, for the ANN5-SH model was 0.972, which is considered excellent [9, 54]). In contrast, the ROC curves

for either category in the ANN5-SD model remained unshifted (from the diagonal, Fig. 3f), and generated an AUC value of 0.587, which is unsatisfactory [9, 54].

Lastly, the importance of the 6 independent variables used to build the ANN5 models was ranked from high to low, those that contributed the most to ANN5-SH were the granularity index of CD11bc/FSC^{high} (100%), Tregs (79.1%), and M2-like macrophages (58.4%) (Fig. 4c). The variables that contributed most to the ANN5-SD model were the M1-like/M2-like ratio (100%), the granularity index of CD11bc/FSC^{high} (88.4%), and Tregs/M1-like ratio (48.5%) (Fig. 4d).

In summary, ANN models built on information from the SH group can correctly classify whether animals were drinking H₂O or NaHCO₃, but one built on the same information from the SD group failed to do so, which is consistent with a splenic nerve role in NaHCO₃-mediated immunoregulation.

Identifying immune markers clusters underlying immunoregulation by principal components analysis (PCA)

In “Effect of oral NaHCO₃ intake in SH and SD animals” and “Effect of spleen denervation on immune markers” we identified interactions between treatment and surgery on several immune markers. We, therefore, wondered whether the immunoregulatory effects of spleen denervation and treatment are differentiated. We use PCA to address this question.

We first ran PCA with the 12 variables including 10 immune markers plus the type of treatment and surgery to examine the correlation matrix, collinearity, and anti-image matrices. Eleven of the 12 variables correlated above 0.3 (Additional file 1: Fig. S5a), 4 variables showed high M1-like multicollinearity coefficients (VIF > 5 and tolerance < 0.2; Additional file 1: Fig. S5b) and one variable (CD11bc + CD38 + cells) had an anti-image correlation matrix below 0.50 (Additional file 1: Fig. S5c). Based

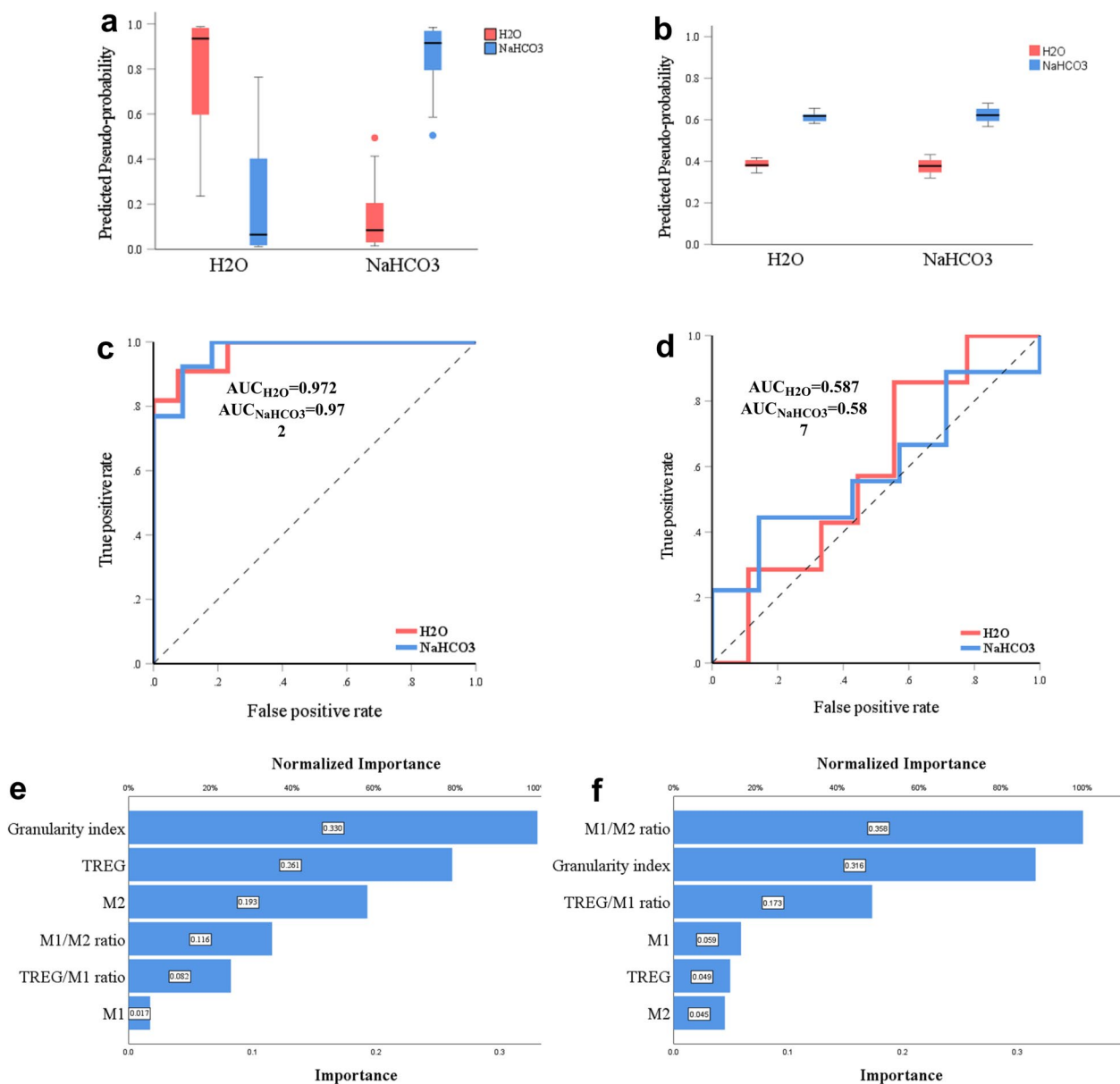


Fig. 4 Predictive pseudoprobability, ROC, and variables' normalized importance for ANN5-SH and ANN5-SD models. **a** The ANN5-SH's predictive pseudo-probability to correctly classify rats drinking H₂O or NaHCO₃ is close to 100%, whereas the misdiagnosed cases were close to zero. **b** The ANN5-SD's predictive pseudo-probability for correct predictions was close to 0.6 (60%) whereas the misdiagnosed cases were at 40%. **c** ANN5-SH's ROC curve, representing the sensitivity (y-axis) and specificity (x-axis) for the model, is supported by an excellent AUC of 0.972. **d** ANN5-SD's ROC curve and an unsatisfactory AUC of 0.587. **e, f** The importance of the 6 independent variables used to build the ANN5 models, **e** corresponds with ANN5-SH and **f** with ANN5-SD. Figure created with SPSS 28 and Prism GraphPad

on this preliminary assessment, we excluded M1-like/M2-like ratio, Treg/M1-like ratio, T-helper, and CD4-T cells and CD11bc+CD38+ cells, keeping 7 variables for further analysis.

A new PCA with the 7 variables shows a Kaiser–Meyer–Olkin (KMO) measure of sampling adequacy of 0.64 (above the recommended value of 0.60) and a

significant Bartlett's test of sphericity ($\chi^2(21) = 59.607, p < 0.001$). Screen plot and parallel test analysis [58, 59] identified two components with eigenvalues over 1.134 (Fig. 5a). The first and second components' eigenvalues explained 33% and 25.5% of the variance respectively, producing a cumulative variance of 58.43% (Table 4). The commonalities are above 0.30 supporting that each variable shares common variance with others (Table 4).

Table 2 Classification is reported as a confusion matrix

Set	SH				SD			
	Prediction				Prediction			
	NaHCO ₃	H ₂ O	Total	Correct (%)	NaHCO ₃	H ₂ O	Total	Correct (%)
Training								
NaHCO ₃	9	0	9	100.0	6	0	6	100.0
H ₂ O	1	6	7	85.7	4	0	4	0.0
Total	10	6	16		10	0	10	
Overall (%)	62.5	37.5		93.8	100.0	0.0		60.0
Testing								
NaHCO ₃	4	0	4	100.0	3	0	3	100.0
H ₂ O	1	3	4	75.0	3	0	3	0.0
Total	5	3	8		6	0	6	
Overall (%)	62.5	37.5		87.5	100.0	0.0		50.0

The correct percentage of cases in the training set for the SH group is 93.8% in comparison with 60.0% in the SD group. For the testing set, the correct percentage predicted by the SH group is 87.5% in comparison with 50% for the SD group

Table 3 Precision, recall, accuracy, and F1 score for ANN-SH and ANN-SD animals' models

	SH		SD	
	Training (%)	Testing (%)	Training (%)	Testing (%)
Precision	90.0	80.0	60.0	50.0
Recall	100.0	100.0	100.0	100.0
Accuracy	93.8	87.5	60.0	50.0
F1 score	94.7	88.9	75.0	66.7

An assessment of the components' structure showed that an orthogonal rotation and quartimax offers the best-defined structure (Fig. 5b). The first component is loaded with Tregs, CD4-FoxP3+ T cells, and M2-like macrophages, in inverse correlation with the presence of spleen denervation (Table 4; orange rectangle in Fig. 5b). The second component is loaded with M1-like macrophages and the granularity index of CD11bc/FSC^{high} cells, both variables in negative correlation with the presence of NaHCO₃ treatment (Table 4; blue rectangle in Fig. 5b). Notably, M2-like macrophages had a cross-loading correlation in both components (Table 4). The PCA's composite reliability to assess internal consistency reliability [21, 79] is 0.837 and 0.769 for components one (4 items) and two (3 items), respectively, which are above 0.7 and considered adequate [1].

Because spleen denervation and NaHCO₃ treatment modulate M2-like macrophages and Tregs, we conduct a PCA only in SH animals. We included the same variables used in the PCA analysis for both groups. For the SH group, the variable CD4-FoxP3+ T cells had an anti-image correlation matrix below 0.50 and was

excluded. The KMO measure of sampling adequacy was 0.73, and Bartlett's test of sphericity was significant ($\chi^2(10) = 43.750, p < 0.001$). The parallel test identified a first component that explained 57.17% of the cumulative variance and had a composite reliability of 0.866 (Table 5). The second identified component minimally contributed to the cumulative variance (Eigenvalue cut-off of 1.233); thus, we retained only the first component. This unique component was loaded (>0.45 loading factor) with the presence of NaHCO₃ treatment, M2-like macrophages, and Treg, in inverse correlation with M1-like macrophages, and the granularity index (Table 5). In contrast, for the SD group, the KMO measure of sampling adequacy was 0.56 (below the recommended value of 0.60) and Bartlett's test of sphericity was not significant ($\chi^2(10) = 6.960, p = 0.729$), thus, we did not carry out further analysis.

Overall, PCA analysis for all animals (SH and SD) treated with NaHCO₃ or H₂O distinguished two distinct clusters of factors underlying immunomodulation, and PCA analysis within the SH group produced a sole component. These analyses are supportive of a multivariate immunomodulatory effect of oral NaHCO₃ treatment.

Discussion

Ray et al. recently demonstrate a decrease in M1-like, and an increase in M2-like macrophages, and Tregs, in rats receiving 0.1-M NaHCO₃ solution for three consecutive days [65]. The authors hypothesize IR activation as the possible mechanism responsible for this effect. Herein, we replicated the NaHCO₃-mediated immunomodulatory effect described by Ray et al. in SH but not in SD animals. Thus, suggesting the necessity of the splenic nerve

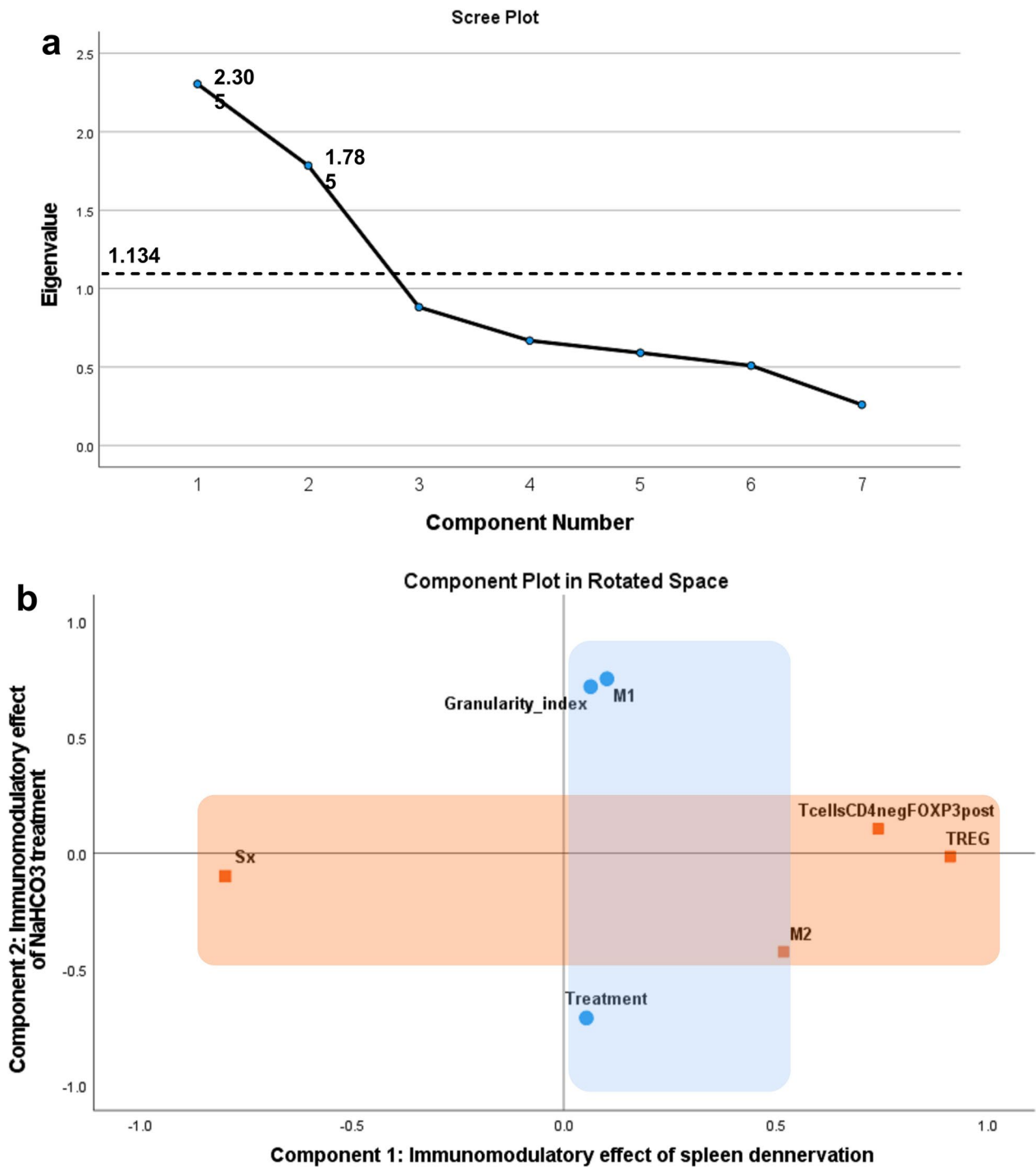


Fig. 5 Principal component analysis (PCA) for SH and SD groups together. **a** Scree plot from PCA showing as many components as variables (x-axis), the parallel analysis for the eigenvalue (y-axis) for component 3 was 1.134 and a dashed line is at that level including only the first two components in the final PCA. **b** The components plot in rotated space including component 1 as an orange area (immunoregulatory effect of spleen denervation) and component 2 as a blue area (immunoregulatory effect of NaHCO₃ treatment). The first component is loaded with Treg, CD4-FoxP3+T cells, M2-like macrophages, and surgery (zero representing sham surgery and one spleen denervation). The second component is loaded with M1-like macrophages, the granularity index, and the treatment (zero representing H₂O and one NaHCO₃ treatment). The area where blue and orange overlap represents the only complex variable in the PCA, which is M2-like macrophages. These cells had a predominant loading factor of 0.518 on Component 1, however, the loading for Component 2 was close to 0.427. Figure created with SPSS 28, and Prism GraphPad

Table 4 The loading factors, communalities, variance, and eigenvalues of PCA combining SH and SD animals in the same group

Variables	Component 1	Component 2	Communalities
PC-unrotated component matrix			
M1-like	0.107	0.748	0.572
M2-like	0.514	-0.431	0.451
Granularity index	0.068	0.715	0.515
Treg	0.911	-0.024	0.831
CD4-FoxP3 + T cells	0.742	0.097	0.560
Surgery	-0.801	-0.096	0.651
Treatment	0.047	-0.713	0.511
PC-rotated component matrix ^a			
M1-like	0.101	0.749	
M2-like	0.518	-0.427	
Granularity index	0.063	0.715	
Treg	0.911	-0.017	
CD4-FoxP3 + Tcells	0.741	0.103	
Surgery	-0.800	-0.102	
Treatment	0.052	-0.713	
Variance			
Proportion of variance (%)	32.932	25.497	
Cumulative variance (%)	32.932	58.429	
Eigenvalue (SD ²)	2.305	1.785	

^a Rotation converged in 3 iterations, rotation method quartimax with Kaiser Normalization; PC, principal component; SD, standard deviation; Factor loadings > 0.50 are bolded

Table 5 Loading factors, communalities, variance, and eigenvalues for PCA for the SH group alone

Variables	Component 1	Communalities
PC-unrotated component matrix		
M1-like	-0.792	0.627
M2-like	0.819	0.671
Granularity index	-0.810	0.656
Treg	0.464	0.215
Treatment	0.830	0.689
Variance		
Proportion of variance (%)	57.174	
Cumulative variance (%)	57.174	
Eigenvalue (SD ²)	2.859	

Factor loadings > 0.45 are bolded

PC principal component, SD standard deviation

to bring about NaHCO₃'s effect. Furthermore, SD, independently from NaHCO₃ treatment, modulated some immune cells whereas others were unaffected. Taken together, these data shed light on the gut-brain-spleen communication responsible for NaHCO₃'s effect on immune-cells-driven anti-inflammatory polarization. In addition to describing a sole immunomodulatory-spleen denervation effect on specific immune cells. To the

best of our knowledge, this is the first evidence that the immunomodulatory effect induced in the spleen by orally ingested NaHCO₃, is mediated by the splenic nerve.

Immunomodulatory effect of oral NaHCO₃ intake in SH animals

Ray et al. hypothesize that the effect of NaHCO₃ in macrophage polarization was by IR activation [65, 66]. In the classic CSAP model [83], upon IR stimulation, CSAP converging into the splenic nerve releases norepinephrine (NE) which activates a subset of T cells in the spleen through β2-adrenergic receptors (β2AR). These T-cells release acetylcholine (ACh) which interact with α7 nicotinic acetylcholine receptors (α7nAChR) in spleen macrophages downregulating the production of proinflammatory cytokines but without increasing IL-10 production [70]. The IR can also be stimulated by splanchnic sympathetic pathways (SAP) which also feed the splenic nerve, increasing IL-10 production [48]. In parallel, NE can also bind to β2AR on macrophages to induce an anti-inflammatory polarization [26], as well as to β2AR on Tregs, proliferation, and enhancing Treg function [19]. Furthermore, the activation of β2-receptors on splenic regulatory lymphocytes via splenic nerve-norepinephrine released upon vagal nerve stimulation

suppresses LPS-induced inflammation, providing additional evidence for the anti-inflammatory properties of these cells [89].

In our study, oral NaHCO_3 modulates M1-like macrophages, M2-like macrophages, Tregs, the ratios of M1-like/M2-like, Tregs/M1-like, and the granularity of CD11bc/ FSC^{high} cells. Other cells were not affected including T-helper, CD11bc+CD38+ cells, CD4-T cells, and CD4-FoxP3+T cells. These results suggest that NaHCO_3 activates the IR.

Notably, we find that among all immunological variables quantified, the largest changes between H_2O and NaHCO_3 groups are observed in Tregs/M1-like and M1-like/M2-like ratios. We anticipate these results based on the single response of M1-like macrophages (suppression), M2-like macrophages (increase), and Tregs (increase) to oral NaHCO_3 (Table 1, Figs. 1, 2). However, the expression of these immune markers as a ratio displays a bigger effect size ($\text{pes}=0.186$, $\text{pes}=0.174$) and significance ($p=0.007$, $p=0.009$) between the treatment groups. Similarly, Ray et al. showed that the monocyte polarization was clearest when expressed as the number of M1-like/M2-like [65, 66]. In the same line, we surmise that the more important difference of Tregs/M1-like and M1-like/M2-like ratios in comparison with M1-like or Treg alone speaks of a functional link between monocytes and Tregs. Macrophages with a more anti-inflammatory phenotype and Tregs seem to regulate each other and generate an immunosuppressive loop through cytokines or cell-to-cell interaction [17, 45, 67, 75, 80, 82].

We found a novel decrease in the granularity index of CD11bc+/ FSC^{high} cells in SH animals treated with NaHCO_3 in comparison with the H_2O group. We distinguished two cell populations based on granularity: agranular (SSC^{low}) and granular (SSC^{high}) and identified CD11bc-positive cells in the latter population, which were the biggest. Previously, a higher proportion of granular than agranular cells has been reported in tumoral cells in an inflammatory environment [47]. The granularity index correlates positively with M1-like and negatively with M2-like macrophages but without collinearity with either macrophage subtype. This suggests that changes in the granularity index of CD11bc+/ FSC^{high} cells move in the same direction as M1-like cells but relying on a different type of cell (lack of collinearity), a potential suggestion is neutrophils. Consistent with this, Ray et al. described a significant decrease in neutrophils (CD16+TNF α +) in the blood of human subjects after a load of oral NaHCO_3 [65].

In addition to finding a sole effect under oral NaHCO_3 intake, where the number of M2-like macrophages and Tregs increase while M1-like and the granularity index

of CD11bc+/ FSC^{high} cells decreases, we also find a multivariate association among these variables with treatment. In SH animals, PCA clusters in one component NaHCO_3 treatment, Tregs, and M2-like macrophages in negative correlation with M1-like macrophages and granularity index of CD11bc+/ FSC^{high} cells. We name this component immunomodulatory effect of NaHCO_3 and suggests an orchestrating immunomodulatory role for NaHCO_3 treatment. As discussed above, the increase in M2-like macrophages increments Tregs, which can further increase M2-like cells. This coordinating effect seems consistent with the notion that NaHCO_3 triggers changes that match the effect of known IR activators [4, 76]. Accordingly, VNS, an established IR activator, reduces neutrophil migration [36], promotes microglial M2-like polarization [15], and reduces lung mRNA levels of M1-like macrophage markers, while increasing M2-like markers [44]. Furthermore, nicotine, another IR activator, reduces neutrophil recruitment during sepsis development [36], and induces both anti-inflammatory macrophage polarization [73] and Tregs number [52].

Splenic nerve and oral NaHCO_3 intake

NaHCO_3 -mediated immunomodulation of immunological markers bespeaks involvement of the IR pathway, but a critical test was to demonstrate the necessity of the splenic nerve to NaHCO_3 's effect. SD animals that received NaHCO_3 treatment did not show changes in M2-like macrophages, M1-like macrophages, granularity index of CD11bc+/ FSC^{high} cells, M1-like/M2-like ratio, Tregs, or Tregs/M1-like ratio. Moreover, ANN analysis correctly classifies whether animals were drinking H_2O or NaHCO_3 only for the SH group but fails to do so for the SD group. As above, a PCA in the SH group gathers M1-like macrophages, granularity index of CD11bc+/ FSC^{high} cells, M2-like macrophages, Tregs, and NaHCO_3 -treatment in one component. However, an attempt to run PCA analysis in SD animals using the same variables fails.

These results demonstrate that the splenic nerve is necessary to observe oral NaHCO_3 -mediated immunomodulatory changes in the spleen. This effect seems independent from the mesothelial cells' choline esterase+ described by Ray et al. [65, 66]. We think so because moving the spleen to the midline of the abdominal cavity was not sufficient to disrupt the immunomodulatory shift seen in SH animals. The splenic nerve is a necessary part of the IR to suppress systemic inflammation. This has been tested in the context of endotoxemia for CSAP and SAP, the efferent arms of the IR. Ballinas-Rosas et al. demonstrated how the splenic nerve was required for CSAP control of TNF α during endotoxemia [69]. Similarly, Martelli et al. report that splenic nerve activity is

dependent on inputs from sympathetic splanchnic nerves during endotoxemia, while is absent when splanchnic nerves have been severed. Moreover, 80% suppression of TNF α is only present in those animals with intact splanchnic nerves [48]. By denervating the spleen, we have disrupted SAP and CSAP as they converge in the splenic nerve. Thus, this finding brings strong support to classify NaHCO₃ as an IR activator.

We have previously suggested a mechanistic model whereby oral NaHCO₃ intake stimulates the IR, in which the immunomodulatory effects of NaHCO₃ might be mediated by choline esterase + mesothelial cells attached to the spleen capsule as well as splenic nerve branches [4]. By stimulating vagal afferents NaHCO₃ oral intake could activate the nucleus of the tractus solitarius and other IR-implicated brain regions, the output of which could trigger the IR via sympathetic (SAP) and parasympathetic (CSAP) pathways converging in the splenic nerve. Additionally, via impacting afferent vagus, NaHCO₃ might stimulate other vagal anti-inflammatory pathways that are not dependent on the spleen [11, 50]. Further experimental assessment within the brain and in animal models of LPS-induced endotoxemia and systemic inflammatory conditions, with disruption of SAP or CSAP, is crucial to validate and refine the characterization of NaHCO₃'s properties as an inflammatory reflex (IR) activator.

Due to successful outcomes in prior studies with inflammatory reflex (IR) activators, NaHCO₃ holds promise for treating various inflammatory conditions, including chronic kidney disease, atherosclerosis, hypertension, coronary artery disease, stroke, cancer, diabetes mellitus type 2 (DM2), obesity, Alzheimer's disease, autoimmune diseases, and psychiatric and neurological disorders [28], Matei, 2022 #618, Annoni, 2019 #619, Li, 2022 #616, Reijmen, 2018 #620, Sorski, 2023 #621, Dai, 2020 #622, Vargas-Caballero, 2022 #623, Ng, 2020 #624, Cimpianu, 2017 #625, [90]. Furthermore, NaHCO₃, commonly used for heartburn and metabolic acidosis, has mild side effects [18] and its role as an IR activator suggests a straightforward translation to clinical use, leveraging its FDA approval and cost-effectiveness. We have recently published a review article that extensively addresses the potential clinical relevance of NaHCO₃ for treating various inflammatory conditions [4].

Spleen denervation has an independent immunomodulatory effect

We found that spleen denervation-independent of H₂O or NaHCO₃ treatment- decreased M1-like macrophages, granularity index in CD11bc/FSC^{high} cells, Tregs, M2-like macrophages, and CD4-FoxP3 + T cells whereas T-helper and CD4-T cells remained unaffected. The effect induced by SD on proinflammatory markers

(M1-like, and granularity index CD11bc + /FSC^{high} cells) was more notable when comparing SH-H₂O with SD-H₂O groups, which was expected as these markers decrease with NaHCO₃ treatment. Contrary, NaHCO₃'s enhancing effect on anti-inflammatory immune markers (M2-like macrophages, and Tregs) sets up a more evident difference between SH and SD animals in the NaHCO₃ group (Table 1). The immunomodulatory SD effect was further evidenced by a PCA component that grouped Tregs, CD4-FoxP3 + T cells, and M2-like macrophages inversely correlated with the presence of spleen denervation.

Consistent with a lower Treg percent in our SD group, an increase in Tregs observed in mice exposed to repeated social defeat stress (RSDS) was abolished in SD animals, which also showed decreased levels of IL-2, IL-17A, and IL-22 (cytokines specific from T cells) whereas T helper cells, IL-6, TNF- α , and IL-10 were unchanged [20]. We also found decreased CD4-FoxP3 + T cells with SD which includes CD8 + FoxP3 + T cells [53]. The function of CD8 + FoxP3 + T cells is not well characterized; however, suppressive properties of CD8 + FoxP3 + T cells in vitro and in vivo have been reported [55], also transcriptomic analysis in murine-induced CD8 + FoxP3 + T cells resembles CD4 + Tregs [3]. Thus, spleen denervation impacts specialized T cells (Tregs, CD4-FoxP3 + T-cells) whereas T-helper and CD4-T cells remain unchanged.

CD11bc + CD38 + cells were increased by spleen denervation. CD38 is present in multiple cell types but is most abundant in hematopoietic cells [63]. In the immune cells, CD38 is expressed in B cells, DC, NK cells, T cells, monocytes, macrophages, and neutrophils among others [63]. This molecule can act as a receptor for CD31 and as a NAD-depleting enzyme having an important role during inflammation [31, 63]. Thus, CD11bc + CD38 + cells in our study may mostly include monocytes, macrophages, DCs, and possibly some NK, B, and T cells, which total number increase by spleen denervation.

A study from Kooijman et al. showed that selective parasympathetic spleen denervation (by clearing connective tissue in the poles of the spleen) increased the count of splenic DC, B cells, and T cells, and gene expression of proinflammatory cytokines in the liver and peritoneal leukocytes in comparison with SH [39]. Additional sympathetic spleen denervation (by clearing of connective tissue in the hilum and splenic arteries) increased circulating IL-1 β and IL-6 [39]. Our surgical spleen denervation combined the two procedures completed by Kooijman et al. We did not measure cytokines, but except for an increase in CD11bc + CD38 + cells (potentially representing monocytes, macrophages, and DCs), the effect in other immune markers suggests a predominant immunosuppressive effect of spleen denervation.

Our data support an independent immunomodulatory effect of SD: it decreased more specialized and polarized cell types such as Tregs, CD4-FoxP3+ T cells, M2-like macrophages; it increased CD11bc+CD38+ cells whereas CD4-T cells and T-helper cells were unaffected. More complete phenotypic panels are needed to better characterize the impact of spleen denervation on these cell populations.

Limitations

Our study has implications but is not without limitations. We did not carry full immunophenotyping for some of the cells reported in the study such as the granularity index of CD11bc+ /FSC^{high} cells, CD11bc+CD38+ cells, and CD4-FoxP3+ T cells which limits and makes the interpretation speculative. We worked with female rats as this sex is predominantly affected by autoimmune and some other inflammatory conditions [6], future work needs to expand our results to males. Also, the multivariate analysis specifically PCA would have benefited from a bigger sample size to conduct confirmatory factor analysis. Despite these limitations, this study contributes to supporting the role of NaHCO₃ as an IR activator which opens a wide broad spectrum of therapeutic possibilities.

Conclusions

We report that the splenic immunomodulatory changes induced by oral NaHCO₃ in SH are abolished in SD animals. This immunomodulatory effect is multivariate, where immune markers are grouped in the same component but proinflammatory cells are polarized on one side, inversely correlating with anti-inflammatory markers and NaHCO₃ treatment located on the opposite side. Thus, further supporting an orchestrating immunoregulatory effect of oral NaHCO₃. To our knowledge, this is the first evidence that the splenic nerve plays a necessary role in communicating signals induced from an oral basic solution to the spleen. This evidence may be enough to classify oral NaHCO₃ as an IR activator. We also report an impact of spleen denervation on splenic immune markers, independent from treatment. This effect was immunosuppressive on more specialized T cells whereas other less specialized ones did not change.

Supplementary Information

The online version contains supplementary material available at <https://doi.org/10.1186/s12974-024-03067-x>.

Additional file 1: Figure S1. Spleen denervation, and flow cytometry protocol. **a.** Cartoon representative of the splenic artery anatomy branching from the celiac artery. The dashed lines show where the surgery was performed at the apical and arterial splenic nerve branches. At the right of the cartoon, there is a complete description of the spleen denervation procedure. Confirmation of spleen denervation was done by western

blot measuring TH protein (SH and SD rats are shown). Sham animals revealed TH whereas SD rats show a decrease or absence of TH. **b.** Flow cytometry protocol details. **Figure S2. Flow cytometry reagents, setup, and percentage rate calculation per cell type.** **a.** List of reagents used for flow cytometry. **b.** Laser lines, emission filters, and fluorochromes were used from Agilent NovoCyte 3000 flow cytometer. Figure created with CorelDraw, Microsoft Office, and Prism GraphPad. **c.** The formulas used to calculate the percentage rate c per cell type after acquisition and gating. **Figure S3. Flow cytometry gating strategy for immune markers was included in the study.** **a.** Flow cytometry gating for spleen macrophages. The number in the lower left corner represents the order of the gates. 1) FSC/SSC gate excludes debris/small particles; 2) FSC-H/FSC-A excludes doublets; 3) gating for alive cells with lower FSC (R3), and higher FSC (R6); 4a) CD11bc+ and lower FSC cells (R17); 4b) CD11bc+ and lower FSC cells (R7); 5a) M1-like macrophages (CD11bc+CD38+TNF α +) and CD11bc+CD38+ cells; 5b) M2-like macrophages (CD11bc+CD206+) cells; 5c) index of the proportion of CD11bc+ higher FSC more granular (SSC^{high}) cells (gate R8), and the proportion of CD11bc+ higher FSC less granular (SSC^{low}) cells (gate R10); 6a) FMO control for M1-like macrophages; 6b) FMO control for M2-like macrophages. **b.** Flow cytometry gating for spleen T cells. 1) Gate for alive CD3+ cells; 2) FSC/SSC gate to exclude debris/small particles; 3) FSC-H/FSC-A to exclude doublets; 4) representative of T-helper, CD4-T cells, Tregs, and CD4-FOXP3+ T cells. All the gates and quadrants include the gated percentage. Almost all gates/quadrants include the number of events except for CD11bc+/CD38+ cells, T helper, CD4-T cells, and the FMO controls. The formula used to calculate a definitive number using negative and positive populations is also included with an arrow pointing to the respective quadrant or gate. Figure created with NovoExpress and Prism GraphPad. **Figure S4. Case processing summary for all AANs and network information for AANs per group.** **A.** Case processing for the ANN models. The random partition for training and testing sets is reflected for each ANN model in SH and SD groups. The model with the most comparable training and setting partition between SH and SD groups is ANN5. **b.** Network information for ANN5-SH and ANN5-SD. **c.** Network architecture for ANN5-SH (left) and ANN5-SD (right). Figure created with SPSS 28, Microsoft PowerPoint, and Prism GraphPad. **Figure S5. Correlation matrix, anti-image matrices, and collinearity statistics.** **a.** Correlation matrix between variables involved in PCA. The 1-tailed significance for the correlation is also reflected. **b.** The collinearity statistics table shows the VIF values. Those variables with VIF >5 such as t-helper, t-cytotoxic, M1-like/M2-like index, and Treg/M1 index were excluded from the PCA analysis. **c.** Anti-image matrices table, the values on the diagonal of the anti-image correlation are all above 0.5 except CD11bc+CD38+ cells which were excluded from PCA. Figure created with SPSSv28 and Prism GraphPad.

Acknowledgements

The authors thank Dr. Mark Stewart for providing insightful feedback throughout all aspects of our study; we thank Dr. Chongmin Huan for his comments on flow cytometry analysis. We thank Dr. Abdoulaye Dabo and Panayiotis Tsokas for their feedback on western blot data. We thank Olaf Welting (The Tytgat Institute for Liver and Intestinal Research at Amsterdam University Medical Center) for his feedback on spleen denervation animal models. We thank The SUNY Animal Facility and Charles River. We also thank Ilse Anton (@science_illustrated_by_ilse) for the design of the graphical abstract.

Author contributions

All authors had full access to all the data in the study and took responsibility for the integrity of the data and the accuracy of the analysis. Milena Rodriguez Alvarez, Juan Marcos Alarcon, Guillem R. Esber, and Christopher A. Roman conceptualized and designed the research. Milena Rodriguez Alvarez, Husam Alkaissi, Laura M. Rodriguez Valencia, Stacy I. Stephenson, and Allison V. Maurice conducted most of the experimental work. Milena Rodriguez Alvarez, Aja M. Rieger, and Christopher A. Roman conducted flow cytometry analysis. Milena Rodriguez Alvarez and Manuel E. Acosta were responsible for the statistical analysis. Milena Rodriguez Alvarez, Juan Marcos Alarcon, Guillem R. Esber, Christopher A. Roman, and Aja R. Rieger were responsible for writing- reviewing, and editing.

Funding

This work was supported by the National Institute on Minority Health and Health Disparities [Grant 5S21MD012474-02]; the National Institute of Neurological Disorders and Stroke [R21NS091830]; and The Empire Clinical Research Investigator Program (ECRIP) scholarship [<https://medicine.buffalo.edu/departments/surgery/research/funding/empire-clinical-research-investigator-program.html>].

Availability of data and materials

This study did not generate new unique reagents. The materials used are available as Additional tables within the study. Detailed data supporting the findings of this study are available from the corresponding author [MRA] on request.

Declarations

Ethical approval and consent to participate

Not applicable.

Competing interests

The authors declare that they do not have any conflicts of interest (financial or otherwise) related to the data presented in this manuscript. All correspondence should be addressed to Milena Rodriguez Alvarez (milena.rodriguezalvarez@downstate.edu).

Author details

¹School of Graduate Studies & Department of Internal Medicine, Division of Rheumatology, SUNY Downstate Health Sciences University, Brooklyn, NY, USA. ²Division of Diabetes, Endocrinology, and Metabolic Diseases, NIH/NIDDK, Bethesda, MD, USA. ³Department of Medical Microbiology and Immunology, University of Alberta, Alberta, Canada. ⁴Center for Studies in Behavioral Neurobiology, Concordia University, Montreal, Canada. ⁵Mathematics and Computer Sciences Department, Barry University, Miami, FL, USA. ⁶Division of Comparative Medicine, SUNY Downstate Health Sciences University, Brooklyn, NY, USA. ⁷Department of Anesthesiology, Downstate Health Sciences University, Brooklyn, NY, USA. ⁸Department of Cell Biology, SUNY Downstate Health Sciences University, Brooklyn, NY, USA. ⁹Department of Rheumatology, SUNY Downstate Health Sciences University, 450 Clarkson Ave, Brooklyn, NY 11203, USA.

Received: 5 January 2024 Accepted: 18 March 2024

Published online: 28 March 2024

References

- Ab Hamid M, Sami W, Sidek MM. Discriminant validity assessment: use of Fornell & Larcker criterion versus HTMT criterion. *J Phys Conf Ser*. 2017.
- Abiodun OI, Jantan A, Omolara AE, Dada KV, Mohamed NA, Arshad H. State-of-the-art in artificial neural network applications: a survey. *Heliyon*. 2018;4(11): e00938.
- Agle K, Vincent BG, Piper C, Belle L, Zhou V, Shlomchik W, Serody JS, Drobycki WR. Bim regulates the survival and suppressive capability of CD8+ FOXP3+ regulatory T cells during murine GVHD. *Blood J Am Soc Hematol*. 2018;132(4):435–47.
- Alvarez MR, Alarcon JM, Roman CA, Lazaro D, Bobrowski-Khoury N, Baena-Caldas GP, Esber GR. Can a basic solution activate the inflammatory reflex? A review of potential mechanisms, opportunities, and challenges. *Pharmacol Res*. 2022; 106525.
- Amici SA, Young NA, Narvaez-Miranda J, Jablonski KA, Arcos J, Rosas L, Papenfuss TL, Torrelles JB, Jarjour WN, Guerau-de-Arellano M. CD38 is robustly induced in human macrophages and monocytes in inflammatory conditions. *Front Immunol*. 2018;9:1593.
- Angum F, Khan T, Kaler J, Siddiqui L, Hussain A. The prevalence of autoimmune disorders in women: a narrative review. *Cureus*. 2020;12(5): e8094. <https://doi.org/10.7759/cureus.8094>.
- Apovian CM, Shah SN, Wolfe BM, Ikramuddin S, Miller CJ, Tweden KS, Billington CJ, Shikora SA. Two-year outcomes of vagal nerve blocking (vBloc) for the treatment of obesity in the recharge trial. *Obes Surg*. 2017;27(1):169–76. <https://doi.org/10.1007/s11695-016-2325-7>.
- Aranow C, Lesser M, Mackay M, Anderson E, Zanos TP, Datta-Chaudhuri T, Bouton C, Tracey KJ, Diamond B. Engaging the Cholinergic Anti-Inflammatory Pathway By Stimulating the Vagus Nerve Reduces Pain and Fatigue in Patients with SLE. *Arthritis Rheumatol*. 2018; 70. WOS:000447268904385.
- Aryadoust V, Goh CC. Predicting listening item difficulty with language complexity measures: A comparative data mining study. *CaMLA Working Papers*. 2014:2014-01
- Badran BW, Austelle CW. The future is noninvasive: a brief review of the evolution and clinical utility of vagus nerve stimulation. *Focus*. 2022;20(1):3–7.
- Bassi GS, Dias DPM, Franchin M, Talbot J, Reis DG, Menezes GB, Castania JA, Garcia-Cairasco N, Resstel LBM, Salgado HC. Modulation of experimental arthritis by vagal sensory and central brain stimulation. *Brain Behav Immun*. 2017;64:330–43.
- Bonaz B, Sinniger V, Hoffmann D, Clarencon D, Mathieu N, Dantzer C, Vercueil L, Picq C, Trocme C, Faure P, Cracowski JL, Pellissier S. Chronic vagus nerve stimulation in Crohn's disease: a 6-month follow-up pilot study. *Neurogastroenterol Motil*. 2016;28(6):948–53. <https://doi.org/10.1111/nmo.12792>.
- Borovikova LV, Ivanova S, Zhang M, Yang H, Botchkina GI, Watkins LR, Wang H, Abumrad N, Eaton JW, Tracey KJ. Vagus nerve stimulation attenuates the systemic inflammatory response to endotoxin. *Nature*. 2000;405(6785):458–62. <https://doi.org/10.1038/35013070>.
- Bremner JD, Gurel NZ, Wittbrodt MT, Shandhi MH, Rapaport MH, Nye JA, Pearce BD, Vaccarino V, Shah AJ, Park J. Application of noninvasive vagal nerve stimulation to stress-related psychiatric disorders. *J Personal Med*. 2020;10(3):119.
- Chen H, Feng Z, Min L, Deng W, Tan M, Hong J, Gong Q, Zhang D, Liu H, Hou J. Vagus nerve stimulation reduces neuroinflammation through microglia polarization regulation to improve functional recovery after spinal cord injury. *Front Neurosci*. 2022; 16.
- de Jonge WJ, van der Zanden EP, The FO, Bijlsma MF, van Westerloo DJ, Bennis RJ, Berthoud HR, Uematsu S, Akira S, van den Wijngaard RM, Boeckstaens GE. Stimulation of the vagus nerve attenuates macrophage activation by activating the Jak2-STAT3 signaling pathway. *Nat Immunol*. 2005;6(8):844–51. <https://doi.org/10.1038/ni1229>.
- Di Benedetto P, Ruscitti P, Vadasz Z, Toubi E, Giacomelli R. Macrophages with regulatory functions, a possible new therapeutic perspective in autoimmune diseases. *Autoimmun Rev*. 2019;18(10): 102369.
- Drugbank (2022). Sodium bicarbonate. <https://go.drugbank.com/drugs/DB01390>.
- Dugger KJ, Chrisman T, Sayner SL, Chastain P, Watson K, Estes R. Beta-2 adrenergic receptors increase TREG cell suppression in an OVA-induced allergic asthma mouse model when mice are moderate aerobically exercised. *BMC Immunol*. 2018;19(1):1–13.
- Elkhatib SK, Moshfegh CM, Watson GF, Schwab AD, Katsurada K, Patel KP, Case AJ. Splenic denervation attenuates repeated social defeat stress-induced T lymphocyte inflammation. *Biol Psychiatry Global Open Sci*. 2021;1(3):190–200.
- Fu Y, Wen Z, Wang Y. A comparison of reliability estimation based on confirmatory factor analysis and exploratory structural equation models. *Educ Psychol Measur*. 2022;82(2):205–24.
- Gaggi M, Repitz A, Riesenhuber S, Aigner C, Sliber C, Fraunschiel M, Cejka G, Sunder-Plassmann G. Effect of oral sodium bicarbonate treatment on 24-hour ambulatory blood pressure measurements in patients with chronic kidney disease and metabolic acidosis. *Front Med*. 2021;8:711034.
- Gonzalez-Gonzalez MA, Bendale GS, Wang K, Wallace GG, Romero-Ortega M. Platinized graphene fiber electrodes uncover direct spleen-vagus communication. *Commun Biol*. 2021;4(1):1–15.
- Gottenberg JE, Morel J, Perrodeau E, Bardin T, Combe B, Dougados M, Flipo RM, Saroux A, Schaefferbeke T, Sibilia J, Soubrier M, Vittecoq O, Baron G, Constantin A, Ravaut P, Mariette X. Comparative effectiveness of rituximab, abatacept, and tocilizumab in adults with rheumatoid arthritis and inadequate response to TNF inhibitors: prospective cohort study. *BMJ*. 2019;364:l67. <https://doi.org/10.1136/bmj.l67>.
- Guarini S, Altavilla D, Cainazzo MM, Giuliani D, Bigiani A, Marini H, Squadrito G, Minutoli L, Bertolini A, Marini R, Adamo EB, Venuti FS, Squadrito F. Efferent vagal fibre stimulation blunts nuclear factor-kappaB activation

- and protects against hypovolemic hemorrhagic shock. *Circulation*. 2003;107(8):1189–94.
26. Guyot M, Simon T, Panzolini C, Ceppo F, Daoullarian D, Murriss E, Macia E, Abelanet S, Sridhar A, Vervoordeldonk MJ, Glaichenhaus N, Blancou P. Apical splenic nerve electrical stimulation discloses an anti-inflammatory pathway relying on adrenergic and nicotinic receptors in myeloid cells. *Brain Behav Immun*. 2019;80:238–46. <https://doi.org/10.1016/j.bbi.2019.03.015>.
 27. Haleem A, Javaid M, Khan IH. Current status and applications of artificial intelligence (AI) in medical field: an overview. *Curr Med Res Pract*. 2019;9(6):231–7.
 28. Hilderman M, Bruchfeld A. The cholinergic anti-inflammatory pathway in chronic kidney disease—review and vagus nerve stimulation clinical pilot study. *Nephrol Dial Transpl*. 2020;35(11):1840–52.
 29. Inoue T, Abe C, Sung SS, Moscalu S, Jankowski J, Huang L, Ye H, Rosin DL, Guyenet PG, Okusa MD. Vagus nerve stimulation mediates protection from kidney ischemia-reperfusion injury through alpha7nAChR+ splenocytes. *J Clin Invest*. 2016;126(5):1939–52. <https://doi.org/10.1172/JCI83658>.
 30. Inoue T, Tanaka S, Okusa MD. Neuroimmune interactions in inflammation and acute kidney injury. *Front Immunol*. 2017;8:945. <https://doi.org/10.3389/fimmu.2017.00945>.
 31. Jablonski KA, Amici SA, Webb LM, Ruiz-Rosado JD, Popovich PG, Partida-Sanchez S, Guerau-de-Arellano M. Novel markers to delineate murine M1 and M2 macrophages. *PLoS ONE*. 2015;10(12): e0145342.
 32. Jaccard J, Turrisi R. Interaction effects in multiple regression. USA: Sage; 2003.
 33. Jantsch J, Schatz V, Friedrich D, Schroder A, Kopp C, Siegelt I, Maronna A, Wendelborn D, Linz P, Binger KJ, Gebhardt M, Heinig M, Neubert P, Fischer F, Teufel S, David JP, Neufert C, Cavallaro A, Rakova N, Kuper C, Beck FX, Neuhofer W, Muller DN, Schuler G, Uder M, Bogdan C, Luft FC, Titze J. Cutaneous Na+ storage strengthens the antimicrobial barrier function of the skin and boosts macrophage-driven host defense. *Cell Metab*. 2015;21(3):493–501. <https://doi.org/10.1016/j.cmet.2015.02.003>.
 34. Ji H, Rabbi MF, Labis B, Pavlov VA, Tracey KJ, Ghia JE. Central cholinergic activation of a vagus nerve-to-spleen circuit alleviates experimental colitis. *Mucosal Immunol*. 2014;7(2):335–47. <https://doi.org/10.1038/mi.2013.52>.
 35. Jossberger H. Toward self-regulated learning in vocational education: difficulties and opportunities. 2011.
 36. Kanashiro A, Hiroki CH, da Fonseca DM, Birbrair A, Ferreira RG, Bassi GS, Fonseca MD, Kusuda R, Cebinelli GCM, da Silva KP. The role of neutrophils in neuro-immune modulation. *Pharmacol Res*. 2020;151: 104580.
 37. Kokol P, Kokol M, Zagoranski S. Machine learning on small size samples: a synthetic knowledge synthesis. *Sci Prog*. 2022;105(1):00368504211029777.
 38. Komisaruk BR, Frangos E. Vagus nerve afferent stimulation: projection into the brain, reflexive physiological, perceptual, and behavioral responses, and clinical relevance. *Auton Neurosci*. 2022;237: 102908.
 39. Kooijman S, Meurs I, van Beek L, Khedoe PP, Giezekamp A, Pike-Overzet K, Cailotto C, van der Vliet J, van Harmelen V, Boeckxstaens G, Berbee JF, Rensen PC. Splenic autonomic denervation increases inflammatory status but does not aggravate atherosclerotic lesion development. *Am J Physiol Heart Circ Physiol*. 2015;309(4):H646–654. <https://doi.org/10.1152/ajpheart.00787.2014>.
 40. Koopman FA, Chavan SS, Miljko S, Grazio S, Sokolovic S, Schuurman PR, Mehta AD, Levine YA, Faltys M, Zitnik R, Tracey KJ, Tak PP. Vagus nerve stimulation inhibits cytokine production and attenuates disease severity in rheumatoid arthritis. *Proc Natl Acad Sci USA*. 2016;113(29):8284–9. <https://doi.org/10.1073/pnas.1605635113>.
 41. Koopman FA, van Maanen MA, Vervoordeldonk MJ, Tak PP. Balancing the autonomic nervous system to reduce inflammation in rheumatoid arthritis. *J Intern Med*. 2017;282(1):64–75. <https://doi.org/10.1111/joim.12626>.
 42. Kwan H, Garzoni L, Liu HL, Cao M, Desrochers A, Fecteau G, Burns P, Frasch MG. Vagus nerve stimulation for treatment of inflammation: systematic review of animal models and clinical studies. *Bioelectron Med*. 2016;3:1–6.
 43. Lapuerta P, Azen SP, LaBree L. Use of neural networks in predicting the risk of coronary artery disease. *Comput Biomed Res*. 1995;28(1):38–52.
 44. Li S, Qi D, Li J-N, Deng X-Y, Wang D-X. Vagus nerve stimulation enhances the cholinergic anti-inflammatory pathway to reduce lung injury in acute respiratory distress syndrome via STAT3. *Cell Death Discov*. 2021;7(1):1–9.
 45. Liu G, Ma H, Qiu L, Li L, Cao Y, Ma J, Zhao Y. Phenotypic and functional switch of macrophages induced by regulatory CD4+ CD25+ T cells in mice. *Immunol Cell Biol*. 2011;89(1):130–42.
 46. Lopez NE, Krzyzaniak M, Costantini TW, De Maio A, Baird A, Eliceiri BP, Coimbra R. Vagal nerve stimulation blocks peritoneal macrophage inflammatory responsiveness after severe burn injury. *Shock*. 2012;38(3):294–300. <https://doi.org/10.1097/SHK.0b013e31825f5fb2>.
 47. Loumagne L, Baudhuin J, Favier B, Montespan F, Carosella ED, Rouas-Freiss N. In vivo evidence that secretion of HLA-G by immunogenic tumor cells allows their evasion from immunosurveillance. *Int J Cancer*. 2014;135(9):2107–17.
 48. Martelli G, Yao ST, McKinley MJ, McAllen RM. Reflex control of inflammation by sympathetic nerves, not the vagus. *J Physiol*. 2014;592(7):1677–86. <https://doi.org/10.1113/jphysiol.2013.268573>.
 49. Martinez FO, Gordon S. The M1 and M2 paradigm of macrophage activation: time for reassessment. *F1000prime Rep*. 2014;6.
 50. Matteoli G, Gomez-Pinilla PJ, Nemethova A, Di Giovangiulio M, Cailotto C, van Bree SH, Michel K, Tracey KJ, Schemann M, Boesmans W. A distinct vagal anti-inflammatory pathway modulates intestinal muscularis resident macrophages independent of the spleen. *Gut*. 2014;63(6):938–48.
 51. McConnell EL, Basit AW, Murdan S. Measurements of rat and mouse gastrointestinal pH, fluid and lymphoid tissue, and implications for in-vivo experiments. *J Pharm Pharmacol*. 2008;60(1):63–70. <https://doi.org/10.1211/jpp.60.1.0008>.
 52. Ménard L, Rola-Pleszczynski M. Nicotine induces T-suppressor cells: modulation by the nicotinic antagonist α -tubocurarine and myasthenic serum. *Clin Immunol Immunopathol*. 1987;44(1):107–13.
 53. Ménoret S, Tesson L, Severine R, Gourain V, Sérazin C, Usal C, Guiffes A, Chenouard V, Ouisse L-H, Gantier M. CD4+ and CD8+ regulatory T cells characterization in the rat using a unique transgenic Foxp3-EGFP model. *bioRxiv*. 2021.
 54. Metz CE. Basic principles of ROC analysis. *Seminars in nuclear medicine*. 1978.
 55. Niederlova V, Tsyklauri O, Chadimova T, Stepanek O. CD8+ Tregs revisited: a heterogeneous population with different phenotypes and properties. *Eur J Immunol*. 2021;51(3):512–30.
 56. Noller CM, Levine YA, Urakov TM, Aronson JP, Nash MS. Vagus nerve stimulation in rodent models: an overview of technical considerations. *Front Neurosci*. 2019;91:461205.
 57. Parrish WR, Rosas-Ballina M, Gallowitsch-Puerta M, Ochani M, Ochani K, Yang LH, Hudson L, Lin X, Patel N, Johnson SM, Chavan S, Goldstein RS, Czura CJ, Miller EJ, Al-Abed Y, Tracey KJ, Pavlov VA. Modulation of TNF release by choline requires alpha7 subunit nicotinic acetylcholine receptor-mediated signaling. *Mol Med*. 2008;14(9–10):567–74. <https://doi.org/10.2119/2008-00079.Parrish>.
 58. Patil V, Singh S, Mishra S, Donavan D. Parallel analysis engine to aid in determining number of factors to retain using R [Computer software]. Spokane, WA, USA: School of Business Administration Spokane, Gonzaga University; 2017.
 59. Patil VH, Singh S, Mishra S, Donavan DT. Efficient theory development and factor retention criteria: abandon the 'Eigenvalue greater than one' criterion. *J Bus Res*. 2008;61(2):162–70.
 60. Pavlov VA, Ochani M, Yang LH, Gallowitsch-Puerta M, Ochani K, Lin X, Levi J, Parrish WR, Rosas-Ballina M, Czura CJ, Larosa GJ, Miller EJ, Tracey KJ, Al-Abed Y. Selective alpha7-nicotinic acetylcholine receptor agonist GTS-21 improves survival in murine endotoxemia and severe sepsis. *Crit Care Med*. 2007;35(4):1139–44. <https://doi.org/10.1097/01.CCM.0000259381.56526.96>.
 61. Pavlov VA, Parrish WR, Rosas-Ballina M, Ochani M, Puerta M, Ochani K, Chavan S, Al-Abed Y, Tracey KJ. Brain acetylcholinesterase activity controls systemic cytokine levels through the cholinergic anti-inflammatory pathway. *Brain Behav Immun*. 2009;23(1):41–5. <https://doi.org/10.1016/j.bbi.2008.06.011>.
 62. Pavlov VA, Tracey KJ. Neural regulation of immunity: molecular mechanisms and clinical translation. *Nat Neurosci*. 2017;20(2):156–66. <https://doi.org/10.1038/nn.4477>.

63. Piedra-Quintero ZL, Wilson Z, Nava P, Guerau-de-Arellano M. CD38: an immunomodulatory molecule in inflammation and autoimmunity. *Front Immunol.* 2020;11: 597959.
64. Rahmatizadeh S, Valizadeh-Haghi S, Dabbagh A. The role of artificial intelligence in management of critical COVID-19 patients. *J Cell Mol Anesthesia.* 2020;5(1):16–22.
65. Ray SC, Baban B, Tucker MA, Seaton AJ, Chang KC, Mannon EC, Sun J, Patel B, Wilson K, Musall JB, Ocasio H, Irsik D, Filosa JA, Sullivan JC, Marshall B, Harris RA, O'Connor PM. Oral NaHCO₃ activates a splenic anti-inflammatory pathway: evidence that cholinergic signals are transmitted via mesothelial cells. *J Immunol.* 2018;200(10):3568–86. <https://doi.org/10.4049/jimmunol.1701605>.
66. Ray SC, Patel B, Irsik DL, Sun J, Ocasio H, Crislip GR, Jin CH, Chen J, Baban B, Polichnowski AJ, O'Connor PM. Sodium bicarbonate loading limits tubular cast formation independent of glomerular injury and proteinuria in Dahl salt-sensitive rats. *Clin Sci (London).* 2018;132(11):1179–97. <https://doi.org/10.1042/CS20171630>.
67. Romano M, Fanelli G, Tan N, Nova-Lamperti E, McGregor R, Lechler RI, Lombardi G, Scottà C. Expanded regulatory T cells induce alternatively activated macrophages with a reduced capacity to expand T helper-17 cells. *Front Immunol.* 2018;9:1625.
68. Ronnback C, Hansson E. The importance and control of low-grade inflammation due to damage of cellular barrier systems that may lead to systemic inflammation. *Front Neurol.* 2019;10:533. <https://doi.org/10.3389/fneur.2019.00533>.
69. Rosas-Ballina M, Ochani M, Parrish WR, Ochani K, Harris YT, Huston JM, Chavan S, Tracey KJ. Splenic nerve is required for cholinergic anti-inflammatory pathway control of TNF in endotoxemia. *Proc Natl Acad Sci USA.* 2008;105(31):11008–13. <https://doi.org/10.1073/pnas.0803237105>.
70. Rosas-Ballina M, Olofsson PS, Ochani M, Valdes-Ferrer SI, Levine YA, Reardon C, Tusche MW, Pavlov VA, Andersson U, Chavan S, Mak TW, Tracey KJ. Acetylcholine-synthesizing T cells relay neural signals in a vagus nerve circuit. *Science.* 2011;334(6052):98–101. <https://doi.org/10.1126/science.1209985>.
71. Rosas-Ballina M, Tracey KJ. The neurology of the immune system: neural reflexes regulate immunity. *Neuron.* 2009;64(1):28–32. <https://doi.org/10.1016/j.neuron.2009.09.039>.
72. Rosas-Ballina M, Valdes-Ferrer SI, Dancho ME, Ochani M, Katz D, Cheng KF, Olofsson PS, Chavan SS, Al-Abed Y, Tracey KJ, Pavlov VA. Xanomeline suppresses excessive pro-inflammatory cytokine responses through neural signal-mediated pathways and improves survival in lethal inflammation. *Brain Behav Immun.* 2015;44:19–27. <https://doi.org/10.1016/j.bbi.2014.07.010>.
73. Saranyutanon S, Acharya S, Deshmukh SK, Khan MA, Singh S, Singh AP. Nicotine causes alternative polarization of macrophages via Src-mediated STAT3 activation: Potential pathobiological implications. *J Cell Physiol.* 2022;237(2):1486–97.
74. Sasaki Y. The truth of the F-measure. *Teach Tutor Mater.* 2007;1(5):1–5.
75. Schmidt A, Zhang XM, Joshi RN, Iqbal S, Wahlund C, Gabrielsson S, Harris RA, Tegnér J. Human macrophages induce CD4+ Foxp3+ regulatory T cells via binding and re-release of TGF-β. *Immunol Cell Biol.* 2016;94(8):747–62.
76. Sharma D, Farrar JD. Adrenergic regulation of immune cell function and inflammation. *Semin Immunopathol.* 2020;42:709–17.
77. Strizova Z, Benesova I, Bartolini R, Novyzedlak R, Cecrdlova E, Foley LK, Striz I. M1/M2 macrophages and their overlaps—myth or reality? *Clin Sci.* 2023;137(15):1067–93.
78. Sugimoto MA, Sousa LP, Pinho V, Perretti M, Teixeira MM. Resolution of inflammation: what controls its onset? *Front Immunol.* 2016;7:160. <https://doi.org/10.3389/fimmu.2016.00160>.
79. Suhr D, Shay M. Guidelines for reliability, confirmatory and exploratory factor analysis. In: Conference proceedings of the Western Users of SAS Software. 2009.
80. Sun S-W, Chen L, Zhou M, Wu J-H, Meng Z-J, Han H-L, Miao S-Y, Zhu C-C, Xiong X-Z. BAMBI regulates macrophages inducing the differentiation of Treg through the TGF-β pathway in chronic obstructive pulmonary disease. *Respir Res.* 2019;20(1):1–10.
81. Tarn J, Legg S, Mitchell S, Simon B, Ng WF. The effects of noninvasive vagus nerve stimulation on fatigue and immune responses in patients with primary Sjogren's syndrome. *Neuromodulation.* 2018. <https://doi.org/10.1111/ner.12879>.
82. Tiemessen MM, Jagger AL, Evans HG, van Herwijnen MJ, John S, Taams LS. CD4+ CD25+ Foxp3+ regulatory T cells induce alternative activation of human monocytes/macrophages. *Proc Natl Acad Sci.* 2007;104(49):19446–51.
83. Tracey KJ. The inflammatory reflex. *Nature.* 2002;420(6917):853–9. <https://doi.org/10.1038/nature01321>.
84. Tracey KJ. Physiology and immunology of the cholinergic antiinflammatory pathway. *J Clin Invest.* 2007;117(2):289–96. <https://doi.org/10.1172/JCI30555>.
85. Tsokas P, Grace EA, Chan P, Ma T, Sealson SC, Iyengar R, Landau EM, Blitzer RD. Local protein synthesis mediates a rapid increase in dendritic elongation factor 1A after induction of late long-term potentiation. *J Neurosci.* 2005;25(24):5833–43.
86. Tsokas P, Hsieh C, Yao Y, Lesburgueres E, Wallace EJC, Tcherepanov A, Jothianandan D, Hartley BR, Pan L, Rivard B. Compensation for PKMζ in long-term potentiation and spatial long-term memory in mutant mice. *Elife.* 2016;5: e14846.
87. Tynan A, Brines M, Chavan SS. Control of inflammation using non-invasive neuromodulation: past, present and promise. *Int Immunol.* 2022;34(2):119–28. <https://doi.org/10.1093/intimm/dxab073>.
88. Veaux RDD, Ungar LH. Multicollinearity: a tale of two nonparametric regressions. In: *Selecting models from data.* New York: Springer; 1994. p. 393–402.
89. Vida G, Pena G, Kanashiro A, del Rocio Thompson-Bonilla M, Palange D, Deitch EA, Ulloa L. β₂-Adrenoreceptors of regulatory lymphocytes are essential for vagal neuromodulation of the innate immune system. *FASEB J.* 2011;25(12):4476.
90. Wang Y, Zhan G, Cai Z, Jiao B, Zhao Y, Li S, Luo A. Vagus nerve stimulation in brain diseases: therapeutic applications and biological mechanisms. *Neurosci Biobehav Rev.* 2021;127:37–53.
91. Wilck N, Balogh A, Marko L, Bartolomaeus H, Muller DN. The role of sodium in modulating immune cell function. *Nat Rev Nephrol.* 2019;15(9):546–58. <https://doi.org/10.1038/s41581-019-0167-y>.
92. Xie F, Yun H, Bernatsky S, Curtis JR. Brief report: risk of gastrointestinal perforation among rheumatoid arthritis patients receiving tofacitinib, tocilizumab, or other biologic treatments. *Arthritis Rheumatol.* 2016;68(11):2612–7. <https://doi.org/10.1002/art.39761>.
93. Yin M, Wortman Vaughan J, Wallach H. Understanding the effect of accuracy on trust in machine learning models. In: *Proceedings of the 2019 Chi conference on human factors in computing systems.* 2019.

Publisher's Note

Springer Nature remains neutral with regard to jurisdictional claims in published maps and institutional affiliations.